

**The Nelson Mandela African Institution of Science and Technology**

**<http://dspace.nm-aist.ac.tz>**

---

Materials, Energy, Water and Environmental Sciences

Masters Theses and Dissertations [MEWES]

---

2020-05

# Charge enhanced capacitive deionization electrodes for deionized water production

Sufiani, Omari

NM-AIST

---

<https://dspace.nm-aist.ac.tz/handle/20.500.12479/974>

*Downloaded from Nelson Mandela-AIST's institutional repository*

**EFFECT OF ELEVATED TEMPERATURE ON PROPERTIES OF  
NEEM SEED HUSK ASH CONCRETE**

**Kizito P. Mwilongo**

**A Dissertation Submitted in Partial Fulfillment of the Requirement for the Degree of  
Master's in Materials Science and Engineering of the Nelson Mandela African  
Institution of Science and Technology**

**Arusha, Tanzania**

**February, 2020**

## **ABSTRACT**

High temperature rise mostly caused by fire is currently becoming a threat that endangers concrete's structural performance for buildings and the safety of dwellers. The behavior of concrete after fire subjection has been of much interest for structural materials design purposes. This study investigated the physical properties and the compressive strength of cement - neem seed husk ash blended concrete exposed to elevated temperatures. The neem seed husk ash was produced by calcining neem seed husks at 800 °C for 6 hours and then sieved through the 125 µm sieve. The cement – neem seed husk ash blended concrete was made by partially replacing cement with 3%, 5%, 7% and 10% of neem seed husk ash. The strength of concrete employed is M25. One hundred and fifty concrete cubes of 150 mm sizes were formed and appropriately cured by immersing in water for 7 and 28 days. The cured concrete cube samples were then exposed to and through targeted different levels of temperature; 25 °C, 200 °C, 400 °C, 600 °C and 800 °C, retained for 3 hours in an electric furnace. It was observed that an optimal replacement of cement by 5% of neem seed husk ash yields concrete with improved fire resistance. The experimental results indicate that the compressive strength of the blended concrete (with 5% of neem seed husk ash) exposed to temperatures up to 400 °C is 21.3% and 23.8% better than the normal concrete at 7 and 28 curing days respectively. Surface cracks and spalling are noticeable at 600 °C for all samples considered in this study.

**Keywords:** Neem seed husk ash, Concrete, Elevated temperature, Spalling, Mass loss, Compressive strength.

## DECLARATION

I, **KIZITO P. MWILONGO** do hereby declare to the Senate of The Nelson Mandela African Institution of Science and Technology that this dissertation is my own original work and that it has neither been submitted nor being concurrently submitted for degree award in any other institution.

---

**Name and signature of candidate**

---

**Date**

The above declaration is confirmed

---

**Name and signature of supervisor 1**

---

**Date**

---

**Name and signature of supervisor 2**

---

**Date**

## **COPYRIGHT**

This dissertation is copyright material protected under the Berne Convention, the Copyright Act of 1999 and other international and national enactments, in that behalf, on intellectual property. It must not be reproduced by any means, in full or in part, except for short extracts in fair dealing; for researcher private study, critical scholarly review or discourse with an acknowledgement, without a written permission of the Deputy Vice Chancellor for Academic, Research and Innovation, on behalf of both the author and The Nelson Mandela African Institution of Science and Technology.

## **CERTIFICATION**

The undersigned certifies that they have read and hereby recommend for acceptance by The Nelson Mandela African Institution of Science and Technology a dissertation entitled; *Effect of Elevated Temperature on Properties of Neem Seed Husk Ash Concrete* in partial fulfillment of the requirement for the degree of Master's in Materials Science and Engineering of The Nelson Mandela African Institution of Science and Technology.

### **Principal supervisor**

Dr. Yusufu Abeid Chande Jande

.....

Signature

.....

Date

### **Co-supervisor**

Dr. Revocatus L. Machunda

.....

Signature

.....

Date

## **ACKNOWLEDGEMENT**

It has been by the grace of God that I have managed to reach this far in my research work. Though most of the influential people are not declared here, I extend my heartfelt appreciation to my family and all who facilitated me to successfully accomplish this research work. May the Almighty God bless the works of their hands.

I humbly appreciate the African Development Bank (AfDB) P-Z1-IA0-016 with grant No. 2100155032816, for offering a full sponsorship for the two years of my studies. I will honor the trust by devoting my time to practicing and promoting science-related carriers to the upcoming generation to realize their contribution.

I express my special thanks and appreciation to Dr. Yusufu A. C. Jande and Dr. Revocatus L. Machunda my supervisors, who took their time to guide me in developing my proposal, carrying out the experimentations as well as writing my manuscript and dissertation as products of this research. The academic and professional inputs from them strengthened me in this academic journey.

I am delighted to give my sincere thanks to Dr. Stephen A. Ntoga my mentor and technical advisor for his tireless efforts in providing some inputs in this study; my fellow students Mr. Amosi Makoye, Mr. Siliacus Salvatory and Ms. Lucia Petro to mention but few, for their support towards this achievement.

I wish also to give my heartfelt appreciation to all teaching and non-teaching staff members, Building Materials Laboratory, Civil Engineering and planning departments in Arusha Technical Collage, Tanzania Atomic Energy Commission (TAEC), University of Dar es Salaam, Lake Cement Ltd for allowing us to access their labs during the materials characterization and experimentation phase of this study.

## **DEDICATION**

The work is dedicated to the Department of Civil Engineering and the Built Environment of the Saint Augustine University of Tanzania (SAUT).



## TABLE OF CONTENTS

ABSTRACT .....	i
DECLARATION .....	ii
COPYRIGHT .....	iii
CERTIFICATION .....	iv
ACKNOWLEDGEMENT .....	v
DEDICATION .....	vi
TABLE OF CONTENTS .....	vii
LIST OF TABLES .....	xi
LIST OF FIGURES .....	xii
LIST OF APPENDICES .....	xiv
LIST OF ABBREVIATIONS AND SYMBOLS .....	xv
CHAPTER ONE .....	1
INTRODUCTION .....	1
1.1 Background of the Problem .....	1
1.2 Statement of the Problem .....	3
1.3 Rationale of the Study .....	3
1.4 Objectives .....	4
1.4.1 General Objective .....	4
1.4.2 Specific Objectives .....	4
1.5 Research Questions .....	4

1.6	Significance of the Study .....	4
1.7	Delineation of the Study.....	5
CHAPTER TWO .....		6
LITERATURE REVIEW .....		6
2.1	Materials for Concrete.....	6
2.1.1	Cementitious Binders .....	6
2.1.2	Hydration of Cement.....	6
2.1.3	Pozzolanic Reaction.....	7
2.1.4	Concrete Aggregates .....	8
2.1.5	Water .....	11
2.2	Properties of Concrete at High Temperatures .....	12
2.3	Mechanical and Physical Properties .....	13
2.4	Properties of Concrete containing Neem Seed Husk Ash.....	14
2.5	Concrete containing Fly Ash at Elevated Temperatures .....	14
CHAPTER THREE.....		17
MATERIALS AND METHODS.....		17
3.1	General Overview .....	17
3.2	Materials .....	17
3.2.1	Cement .....	17
3.2.2	Coarse Aggregates .....	18
3.2.3	Fine Aggregates .....	19

3.2.4	Water .....	20
3.2.5	Neem Seed Husk Ash .....	20
3.3	Experimental Procedures.....	20
3.3.1	Preparation of Neem Seed Husk Ash.....	20
3.3.2	Characterization of Neem Seem Husk Ash.....	21
3.3.3	Properties of Aggregates .....	21
3.3.4	Mix Design Methods for Concrete .....	23
3.3.5	Concrete Mix Proportions .....	24
3.3.6	Production of Concrete .....	24
3.3.7	Workability of Concrete.....	25
3.3.8	Preparation of Concrete Specimens .....	27
3.3.9	Thermal Treatment.....	27
3.3.10	Testing Program.....	28
CHAPTER FOUR.....		30
RESULTS AND DISCUSSION.....		30
4.1	Properties of Aggregates .....	30
4.2	Production of Neem Seed Husk Ash.....	31
4.2.1	Thermogravimetric Analysis .....	31
4.2.2	Characterization of Neem Seed Husk Ash.....	32
4.2.3	Gradation of Neem Seed Husk Ash.....	34
4.3	Properties of Fresh Concrete .....	34

4.4	Properties of Hardened Concrete.....	35
4.4.1	Physical Characteristics with Temperature Rise .....	35
4.4.2	Spalling and Mass Loss.....	37
4.4.3	Residual Compressive Strength.....	39
CHAPTER FIVE .....		46
CONCLUSION AND RECOMMENDATIONS .....		46
5.1	Conclusion.....	46
5.2	Recommendations.....	47
REFERENCES .....		49
RESEARCH OUTPUTS .....		68

## LIST OF TABLES

Table 1: ASTM C618 Chemical Requirements .....	7
Table 2: Commonly used sieve designation and the corresponding opening size .....	10
Table 3: Chemical composition of cement .....	18
Table 4: The designed concrete mix proportions .....	24
Table 5: Measured properties of aggregates .....	30
Table 6: XRF and BET results .....	33
Table 7: Physical characteristics of concrete mixes at elevated temperatures .....	36
Table 8: Residual compressive strength for the 7 and 28 days cured concrete samples .....	40
Table 9: Approximate compressive strengths ( $\text{N/mm}^2$ ) of concrete mixes made with a free water/cement ratio of 0.5 .....	61
Table 10: Approximate free-water contents ( $\text{kg/m}^3$ ) for various levels of workability .....	64
Table 11: Minimum cement content requirement .....	65

## LIST OF FIGURES

Figure 1:	Five types of aggregate gradation (Neville & Brooks, 2010) .....	10
Figure 2:	Coarse aggregates .....	19
Figure 3:	Fine aggregates .....	19
Figure 4:	The NSHA used in this study .....	20
Figure 5:	The NSHA produced at different calcination temperatures .....	21
Figure 6:	Concrete production .....	25
Figure 7:	Slump testing: (a) temping (b) surface leveling (c) slumping (d) slump measurement .....	26
Figure 8:	Sample preparation: (a) molds; (b) casting; (c) demolding; and (d) curing .....	27
Figure 9:	Thermal treatment for concrete cubes: (a) heating, and (b) cooled sample .....	28
Figure 10:	Compressive strength testing machine .....	29
Figure 11:	Particle size distribution of the used aggregates .....	31
Figure 12:	The TGA curve for the neem seed husks .....	32
Figure 13:	Particle size distribution of NSHA .....	34
Figure 14:	Slump values for all concrete batches .....	35
Figure 15:	Mass loss versus temperature for OPC and NSHA concrete cured for 7 days .....	38
Figure 16:	Mass loss versus temperature for OPC and NSHA concrete cured for 28 days .....	39
Figure 17:	Residual compressive strength versus temperature for the 7 days cured concrete ...	41
Figure 18:	The ratio of residual compressive strength for the 7 days cured concrete .....	42
Figure 19:	Residual compressive strength versus temperature for the 28 days cured concrete ..	43

Figure 20: The ratio of residual compressive strength for the 28 days cured concrete .....	44
Figure 21: Relationship between standard deviation and characteristic strength; BSI (1986) – Fig. 3 .....	62
Figure 22: Relationship between compressive strength and free-water/cement ratio BSI (1986) – Fig. 4 .....	63
Figure 23: Estimated wet density of fully compacted concrete; BSI (1986) – Fig. 5 .....	66
Figure 24: Recommended proportions of fine aggregate according to percentage passing a 600 $\mu\text{m}$ sieve; (BSI (1986)) – Fig.6 .....	67

## **LIST OF APPENDICES**

Appendix 1: Preparation of NSHA .....	57
Appendix 2: Moisture content and bulk density of aggregates .....	58
Appendix 3: Water absorption and the specific gravity of aggregates .....	59
Appendix 4: Particle size distribution of aggregates .....	60
Appendix 5: Detailed concrete mix design calculations .....	61



## LIST OF ABBREVIATIONS AND SYMBOLS

AD	Air Dry
ASTM	American Society for Testing and Materials
BET	Brunauer-Emmett-Teller
C <sub>2</sub> S	Dicalcium Silicate
C <sub>3</sub> A	Tricalcium Aluminate
C <sub>3</sub> S	Tricalcium Silicate
C <sub>4</sub> AF	Tetracalcium Aluminoferrite
C-H	Calcium Hydroxide
C-S-H	Calcium Silicate Hydrates
DTA	Differential Thermal Analysis
$G_s$	Specific Gravity
LoI	Loss on Ignition
NSHA	Neem Seed Husk Ash
OD	Oven-Dry
OPC	Ordinary Portland Cement
PFA	Pulverized Fly Ash
POFA	Palm Oil Fuel Ash
RHA	Rice Husk Ash
SCBA	Sugar Cane Bagasse Ash
SCMs	Supplementary Cementitious Materials

SSD	Saturated Surface Dry
TGA	Thermogravimetric Analysis
XRF	X-Ray Fluorescence

## CHAPTER ONE

### INTRODUCTION

#### 1.1 Background of the Problem

Concrete is a composite building material comprised of coarse and fine aggregates glued together with cement paste which upon hardening results in the desired structure. It is a material of choice for applications that require high-temperature-resistant materials (Abid, Hou, Zheng & Hussain, 2017). However, concrete structures can only serve the intended purpose provided that the threshold point is not exceeded upon exposing them to elevated temperatures like in case of fire accidents (Parthasarathi, Saraf, Prakash & Satyanarayanan, 2019).

The current development of infrastructures due to urbanization consumes about 11 billion tons of concrete yearly and is likely to exceed 18 billion tons by the year 2050 (Naqi & Jang, 2019). This implies that its raw materials, more particularly cement are highly consumed. It is reported that in every ton of ordinary Portland cement (OPC) manufactured nearly 900 kg of CO<sub>2</sub> is also produced contributing to about 7% of the entire CO<sub>2</sub> emissions worldwide (Turner & Collins, 2013). Hence, the issue of materials sustainability and environmental pollution accelerated by the concrete industry need to be addressed. Many researchers of our century have been looking for eco-friendly materials that can partially or totally substitute cement in the mix with the aim of handling the raised concern on depletion of raw materials, atmospheric pollution, global warming and waste disposal (Khaliq & Mujeeb, 2019). However, such replacement should result in improved strength and durability properties of concrete.

Currently, pozzolans from agro-wastes and industrial wastes have been of much interest in the field of building materials as they contribute to blended cement concrete with superior properties parallel to the reduction of the aforementioned environmental problems (Ismail, Ismail & Muhammad, 2011). With the growing interest in looking for eco-friendly building materials, researchers found a need for assessing the potential use of ash from agricultural wastes. Several studies have been performed to assess the properties of blended concrete at normal and elevated temperatures utilizing rice husk ash (Haloob, 2011; Gursel, Maryman & Ostertag, 2016; Mboya, King'onde, Njau & Mrema, 2017), palm oil fuel ash (Tangchirapat,

Saeting, Jaturapitakkul, Kiattikomol & Siripanichgorn, 2007; Awal & Shehu, 2015), and sugar cane bagasse ash (Bahurudeen, Kanraj, Dev & Santhanam, 2015; Gar, Suresh & Bindiganavile, 2017) as admixtures in concrete production. The blended concrete was observed to have better performance than normal concrete resulting from the presence of amorphous silica in the aforementioned synthetic pozzolanic materials (Aprianti, Shafigh, Bahri & Farahani, 2015; Khaliq & Mujeeb, 2019). Therefore, studies need to be done to look for more materials with good properties which can result in sustainable and improved concrete products. For example, the increasing world's demand for fuel has led more researchers to look for biodiesel from neem seeds which also produce a large number of wastes (Ali, Mashud, Rubel & Ahmad, 2013). These wastes have a potential application as eco-friendly building materials since neem seed husk ash (NSHA) has good pozzolanic properties and can partially substitute cement in normal strength concrete (Musa & Ejeh, 2012; Musa, 2014; Ibiwoye & Naalla, 2017; Raheem & Ibiwoye, 2018). However, materials used in concrete structures must meet certified fire-resisting constraints as stipulated by the assorted standards subject to the intended structural purpose (EN, 2002).

Meanwhile, there are complications on the fire endurance ability of traditional concrete by itself due to dissimilar thermal characteristics of the components forming the composite material, porosity and moisture content (Ismail *et al.*, 2011). However, structural products from OPC are generally considered as mold fire-resisting materials that can still perform suitably even after a long time of exposure (Savva, Manita & Sideris, 2005). According to Khoury (1992) with careful selection of materials, we can retain the compressive strength of conventional concrete without substantial loss up to around 550 °C - 600 °C temperature rise. However, for exposures exceeding 200 °C, concrete's internal stresses are high enough to cause cracking and notable damages which eventually leads to decreased compressive strength. It is, therefore, essential to examine the properties of blended concrete to have a clear knowledge of the emerging materials before they are incorporated in concrete production. Since many factors like age of concrete, the inclusion of pozzolanic materials and type of aggregates used (Hager, 2013) all together influence the strength and macro properties of concrete at raised temperatures; it is, therefore, important to examine the residual compressive strength for concrete under such exposures for structural safety (Owaid, Hamid & Taha, 2016). A good number of available studies concentrated on assessing the influence of exposure time, the methods of cooling and loading behaviors on

the mechanical properties of concrete incorporating the processed pozzolanic materials from agro wastes like rice husk ash (Wang, Meng & Wang, 2017; Umasabor & Okovido, 2018), palm oil fuel ash (Ismail *et al.*, 2011), bamboo ash (Ishak *et al.*, 2019), and sugar cane bagasse ash (Gar *et al.*, 2017) subjected to elevated temperatures. Unlike previous studies, this study intends to investigate the residual compressive strength and physical response of blended cement concrete containing NSHA as pozzolanic materials after exposure to elevated temperatures up to 800 °C. A comparison is then made on residual strength and physical properties of NSHA concrete with those of the conventional concrete.

## **1.2 Statement of the Problem**

Properties of composite materials like concrete under different environments are complex due to dissimilar properties of individual constituent materials. However, concrete produced with the application of some admixtures has shown to behave differently under varying exposure conditions. Synthetic pozzolanic materials from agro-wastes have acquired great attention from many researchers in our time. The growing interest in producing biodiesel from neem seeds has led to the accumulation of biowastes which has been proven to be a suitable concrete admixture. There are some studies which investigated the properties of concrete containing NSHA at ordinary temperatures (Musa, 2013; Ibiwoye & Naalla, 2017; Raheem & Ibiwoye, 2018). However, no information is available on the properties of NSHA concrete at elevated temperatures. The current study, therefore, aims at providing experimental results of some physical and mechanical properties of NSHA concrete exposed to high temperatures up to 800 °C.

## **1.3 Rationale of the Study**

The current challenges facing the world like global warming, depletion of raw materials and environmental pollution originating from industrial activities need alternative eco-friendly materials. With the advancement in technology, fire accidents are reported to be a threat to structures like buildings. The structural integrity of concrete elements deteriorates when exposed to high temperatures (Chen, Li & Chen, 2009; Morsy, Alsayed & Aqel, 2010). There is, therefore, a need to examine the behavior of concrete that incorporates emerging materials at elevated temperatures to have a clear knowledge of their response before they are fully applied in construction to ensure the safety of the occupants.

## **1.4 Objectives**

### **1.4.1 General Objective**

The current study mainly aims at investigating the properties of neem seed husk ash concrete exposed to elevated temperatures.

### **1.4.2 Specific Objectives**

- i. To select and proportion the concrete ingredients.
- ii. To assess the suitable conditions for neem seed husk ash production from neem seed husks.
- iii. To assess the physical and mechanical properties of neem seed husk ash concrete exposed to high temperatures (up to 800 °C).

## **1.5 Research Questions**

- i. What are the properties of concrete ingredients to be used for design purposes?
- ii. What is the optimum calcination temperature of neem seed husks for NSHA production?
- iii. What is the maximum safe temperature to which the structural concrete containing NSHA can still possess the desirable physical and mechanical properties to carry the design load?

## **1.6 Significance of the Study**

Generally, all engineering structures are designed for safety and economic factors. It is, therefore, necessary to have a clear understanding of all construction materials before they are recommended for applications. This study aimed at providing knowledge on the behavior of NSHA concrete when exposed to elevated temperatures. A clear understanding of NSHA materials in concrete will attract their application in the construction industry thereby producing concrete products with superior properties as well as controlling environmental pollution.

## **1.7 Delineation of the Study**

The study was based on the experimental investigation of the properties of concrete containing the NSHA (as mineral admixture) exposed to elevated temperatures. The first part of this experimental work concentrated on producing the NSHA from neem seed husks, agricultural wastes in a lab-scale by calcining them using an electric furnace. Thermogravimetric analysis (TGA) was done on the neem seed husks sample to determine the suitable range of calcination temperatures. Based on the TGA results, different temperatures were considered for the production of NSHA, from which elemental analysis justified the optimal calcination temperature to produce NSHA with maximum pozzolanic activity. The second part of this study was investigating the properties of concrete containing NSHA subjected to elevated temperatures. A fixed heating rate of 10 °C/min using an electric furnace was adopted and the samples were allowed to cool within the furnace. Physical characteristics (surface cracks and spalling) of the heated samples were visually assessed. The masses of all samples were recorded before and after thermal treatment from which the mass loss was calculated. The compressive strength was determined from the concrete samples for each batch considered.

## **CHAPTER TWO**

### **LITERATURE REVIEW**

#### **2.1 Materials for Concrete**

##### **2.1.1 Cementitious Binders**

Binders can be classified depending on their composition as either organic or inorganic. The organic binders can easily be burnt and hence are not suitable for structures that need to withstand fire. Good examples of common organic binders used are polymer and asphalt. However, inorganic binders normally comprise of various natural minerals. They occur in two different forms as those which may harden in water (hydraulic cement) and the ones which don't need water in the hardening process to gain strength (anhydrous cement) as in case of lime and gypsum. The two categories of inorganic cement mainly differ in composition; hydraulic cement comprises silicate matters (clayey impurities). Portland cement (PC), hydraulic lime, and pozzolan cement are examples of hydraulic cement. Most of the civil engineering applications over many years make use of hydraulic cement. The OPC consists of the following main chemical components; tricalcium silicate ( $C_3S$ ); tricalcium aluminate ( $C_3A$ ); dicalcium silicate ( $C_2S$ ); and tetracalcium aluminoferrite ( $C_4AF$ ) (Kurdowski, 2014). About 68 to 75% of PC is occupied by  $C_3S$  and  $C_2S$ . Hence, PC can then be described as a material that blends CaO and  $SiO_2$  in a ratio that results in calcium silicate which will react chemically with water at standard temperature and pressure (Gambhir, 2013).

##### **2.1.2 Hydration of Cement**

The process by which the main compounds of cement chemically react with water to yield calcium silicate hydrate (C-S-H) gel and calcium hydroxide (CH) is termed as hydration. Various solid phases are formed when the main cement minerals hydrate at different rates. The phases formed are the ones influencing the strength of the formed cement paste (Gartner, Young, Damidot & Jawed, 2002). The hydration process of the calcium silicate minerals present in the OPC highly influences the strength of formed cement paste. The early concrete strength is an outcome of the hydration of  $C_3S$ , which is the most plentiful and important mineral in OPC. The hydration of  $C_2S$  has little influence on the early strength



but substantially contribute to their mature age paste strength (Gambhir, 2013). The hydration of both  $C_3S$  and  $C_2S$  yields the same products which are the C-S-H gel phase and CH as presented in equations (1) and (2) (Scrivener, Juilland & Monteiro, 2015). However, the free lime (CH) produced by  $C_2S$  is relatively less because of less solubility of  $C_2S$  leading to a slow rate of hydration reaction compared to  $C_3S$ .



### 2.1.3 Pozzolanic Reaction

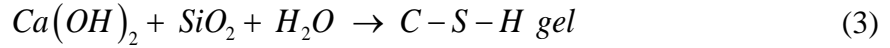
Pozzolans are either natural or manmade alumino-silicate materials which can be applied in mortar mixtures as a replacement of cement. These materials can react with calcium hydroxide (free lime) yielded in the hydration of cement under the moistured condition to produce a highly cementitious reaction product, C-S-H gel, at ordinary temperatures. Silica fume and fly ashes are the commonly applied pozzolans in novel Portland cement. Ashes from the combustion of agro-wastes have shown to have good pozzolanic properties and are highly recommended for application (Aprianti *et al.*, 2015). The principal chemical components are the oxides of silicon and aluminium metals. Some chemical requirements are necessary for pozzolans to be considered as supplementary cementitious material as specified by part C618 of the American Society for Testing and Materials (ASTM) as indicated in Table 1.

Table 1: ASTM C618 Chemical Requirements

	Class		
	N	F	C
Silicon dioxide ( $SiO_2$ ) plus aluminum oxide ( $Al_2O_3$ )	70	70	50
plus iron oxide ( $Fe_2O_3$ ), min %			
Sulfur trioxide ( $SO_3$ ), max, %	4.0	5.0	5.0
Moisture content, max, %	3.0	3.0	3.0
Loss on Ignition (LoI), max, %	10.0	6.0	6.0

The free lime produced as shown in the equation (1) does not participate much in the development of cement paste strength. Moreover,  $Ca(OH)_2$  is prone to leaching from the

hydrated cement paste, thus negatively affecting the durability of concrete. The silicon dioxide from the pozzolans react with  $\text{Ca(OH)}_2$  to yield C-S-H gel, the principal binding agent in cement. This manner is described in equation (3) (Shetty, 2000; Kurdowski, 2014).



The benefit of using these materials is that they result in green cement products at a relatively low cost. Pozzolans can substitute clinkers in the cement production phase thereby reducing  $\text{CO}_2$  emissions (Gambhir, 2013).

#### **2.1.4 Concrete Aggregates**

The properties of both fresh and hardened concrete highly depend on aggregates used as they compose a skeleton of concrete. For the normal concrete about three-quarters of its volume constitute aggregates. They actively affect concrete's performance through their physical, thermal and in some cases chemical properties (Shetty, 2000).

##### **i. Effect of Aggregates**

Aggregates as the basic unit of concrete are responsible for producing a dimensionally stable, durable, workable, elastic and cost-effective concrete. Among other features; the shape and texture of aggregates affect the properties of concrete. Aggregates' shape influences the workability property of concrete whereas the surface texture affects the strength of concrete through the aggregates-matrix bond. Generally, crushed aggregates are more preferred than the uncrushed ones as they are characterized by having particles with angular rough surface textures which result in a low workable but higher strength concrete (Gambhir, 2013).

##### **ii. Classification of Aggregates**

Aggregates can be classified depending on the source, size, and unit weight. According to their size, aggregates of either source or unit weight are classified either as coarse aggregates (CA) or fine aggregates (FA). The retained aggregates on a 4.75 mm sieve are classified as CA and their size ranges from 5 to 150 mm. However, for structural applications employing the normal concrete CA having a maximum size of about 25 mm is recommended whereas no more than 150 mm size can be applied for mass concrete in dams and deep foundation

applications. The fine aggregates are the particles which freely pass through a 4.75 mm sieve and predominately retained on a 75  $\mu\text{m}$  sieve (EN, 1992).

### **iii. Moisture Conditions**

This property describes the extent of water existing on the surface and in the pores of the aggregates. Four conditions of moisture exist as oven-dry (OD), air dry (AD), saturated surface dry (SSD) and wet. The OD is found by driving all pore water to attain a constant weight by maintaining them at a temperature of 110 °C in an oven. Air dry describes a state at which the pores are partially filled with water for aggregates kept in an ambient environment. The properties need to be determined as aggregates existing in either the OD or AD state they will take up water in the process of concrete making until they get saturated. Saturated surface dry describes a state in which the pores available in the aggregate are totally occupied with water while the surface remains dry. The coarse aggregates are submerged for 24 hours in water and then dried by wrapping the surface using a wet cloth. In designing the concrete mix, SSD is considered as the standard index since at the mixing stage water is neither absorbed nor given out by aggregates. Aggregates in wet conditions are characterized by pores filled with water and water films on their surfaces. They are likely to add up water in the system during the process of producing concrete (Gambhir, 2013).

### **iv. Grading of Aggregates**

The workability of fresh concrete is highly influenced by the number of voids among aggregate particles that need to be filled up with an equivalent volume of cement paste (Neville & Brooks, 2010). Sieve analysis is usually done to obtain the aggregates' grading curve for proper selection of the suitable aggregates to be used. Table 2 presents the commonly used sieves.

Table 2: Commonly used sieve designation and the corresponding opening size

Sieve Designation	Nominal Size of Sieve Opening
6 in.	150 mm
3 in.	75 mm
1.5 in.	37.5 mm
3/4 in.	19 mm
3/8 in.	9.5 mm
No. 4	4.75 mm
No. 8	2.36 mm
No. 16	1.18 mm
No. 30	600 $\mu\text{m}$
No. 50	300 $\mu\text{m}$
No. 100	150 $\mu\text{m}$
No. 200	75 $\mu\text{m}$

Neville & Brooks (2010)

The standard curves describing the aggregates' size distribution are explained in Fig. 1. The dense and well-graded types represent a smooth distribution with a wide range of sizes, and they are suitable for concrete production. They describe coarse and fine aggregates respectively.

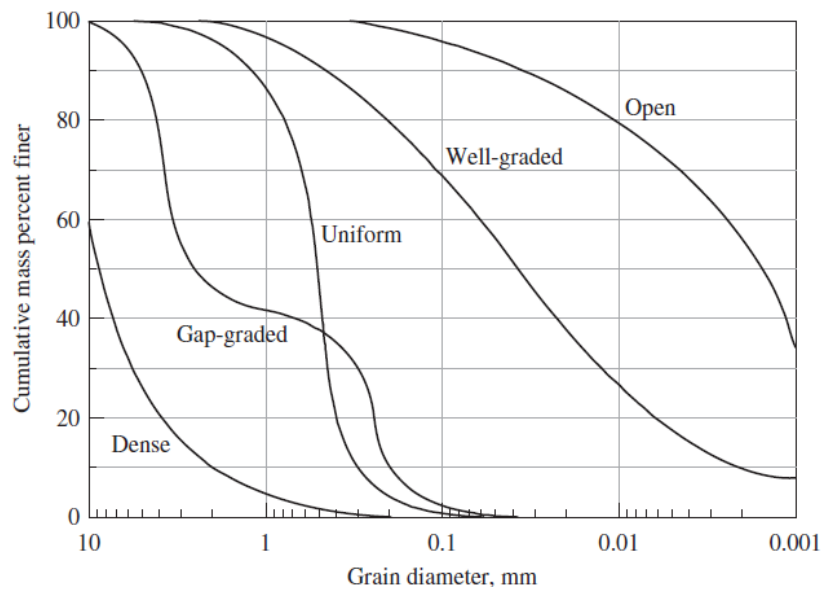


Figure 1: Five types of aggregate gradation (Neville & Brooks, 2010)

Gap graded distribution indicates the absence of certain intermediary size as characterized by a region that is nearly horizontally flat along the curve. In a uniformly distributed grading, only certain size ranges dominate the largest part of the materials, as indicated by a nearly vertical curve at the size which dominates. However, in open grading voids between aggregates are relatively large as the undersized aggregates overshadow the bulk and may

easily be dislocated by a small opening. Such materials are not recommended for construction activities as they result in weak concrete (Neville & Brooks, 2010; Gambhir, 2013).

**v. Fineness Modulus**

The general description aggregates basing on how coarse or fine they are, the idea of a fineness modulus is utilized. The equation 4 defines the fineness modulus (FM).

$$FM = \frac{\sum(\text{cumulative retained percentage on specified sieves})}{100} \quad (4)$$

A series of sieves from 6 in to No. 100 as described in Table 2 are specifically used for calculating the fineness modulus of aggregates. The value of fineness modulus should lie between 2.3 and 3.1 for fine aggregates. Coarse materials will be indicated by a larger number whereas fine materials will be described by a small number. Low fineness modulus requires more paste to become workable. The fineness modulus is, therefore, necessary to be determined for the fine aggregates to be used in the proportioning phase as the concrete's workability will highly be influenced by it (Duggal, 2008).

**2.1.5 Water**

Water is an essential ingredient of concrete that usually occupies 15 to 25% by volume of a properly designed concrete mixture (Gambhir, 2013; Kurdowski, 2014). It is responsible for producing the chosen properties of the fresh as well as the hardened concrete state. In the concrete production process, water plays a vital role in mixing, curing and washing the aggregates as described below:

**i. Mixing Water**

It is the amount of water which interacts with cement, and affects the slump value of concrete; it also controls the long term properties of concrete (strength and durability). Water will only be considered suitable for concrete production if it is free from chemical contaminations and safe for human consumption (Gambhir, 2013). It is meant to perform three main functions: firstly it initiates the hydration reaction of cement to produce the hydration products which provide the binding; secondly, it also contributes to a workable

fresh concrete mixture by lubricating the ingredients involved to produce concrete; and finally, it acquires the required gap within the paste for the improvement of hydration products (Li, 2011). Practically, the quantity of water necessary for satisfactory workability exceeds that required for full cement hydration.

## **ii. Water for Curing of Concrete**

Due to comparatively short contact time between the curing water and the concrete, water required in this case has fewer restrictions than for the case of mixing water. For this purpose, water containing organic and inorganic matters, acids and chlorides may be used particularly when minor discoloration on the surface of the concrete is not objectionable. However, the impurities must be within acceptable limits (Kurdowski, 2014).

## **iii. Water for Washing Aggregate**

Aggregates for concrete production are washed to remove all organic and clayey materials coated on their surfaces, which when left might interrupt the bonding behavior with the cement paste. Water which is free from materials that can generate detrimental films or coats on the surfaces of aggregate particles is considered suitable for washing the aggregates (Duggal, 2008).

## **2.2 Properties of Concrete at High Temperatures**

The response of concrete structures, when exposed to fire, depends on the mechanical, thermal, and deformation behavior of concrete. Such properties vary considerably with temperature, chemical composition and the features of ingredients used in producing the concrete mix batch, heating rate and some other conditions of the surrounding environment (Kodur, 2014). As pointed out earlier, concrete is considered advantageous among other construction materials as it possesses good fire-resistant properties despite being not a refractory material. The fire resistance behavior of concrete is governed by its capacity to endure heat and the later action of water with no strength loss, its thermal conductivity and its coefficient of thermal expansion (Kong, Huang, Corr, Yang & Shah, 2018). The concrete is stable in terms of strength at temperatures up to about 250 °C; however, a definite strength loss occurs at temperatures greater than 300 °C. Normally 70 – 80% of a matured cement paste is occupied by layered C-S-H gel whereas 20% is occupied by the portlandite

(Ca(OH)<sub>2</sub>), and some other chemical compounds. According to Horszczaruk, Sikora, Cendrowski and Mijowska (2017), there is a significant amount of free lime (Ca(OH)<sub>2</sub>) in hydrated mature concrete from which its water gets lost for temperatures beyond 400 °C. Daniel and Sanjayan (2010) observed the decomposition of portlandite between 450 °C and 550 °C temperature rise. Such decomposition results in the production of calcium oxide (CaO). The C-S-H phases of the hardened concrete decompose at temperatures ranging between 600 °C and 700 °C to form C<sub>2</sub>S. Apart from the temperature and pressure, decomposition also depends on the amount of SiO<sub>2</sub> available in the limestone. Concrete melts at temperatures above 1200 °C and up to 1300 °C (Khoury, 2000).

### **2.3 Mechanical and Physical Properties**

Concrete's behavior in fire is dependent on its constituents and mix proportions. The failure in concrete structures subjected to fire differs depending on the type of fire, the system of loading and the nature of the structure. Failure might happen from either loss of tensile, bond, torsional, and compressive strength or concrete spalling (Ma, Guo, Zhao, Lin & He, 2015). At elevated temperatures, the mechanical properties that govern the fire resistance of concrete elements are the compressive and tensile strength, modulus of elasticity, and the stress-strain response of ingredient materials. Unlike most of the materials, the thermal properties of concrete (a composite material) are complicated because not only are characterized by different properties of the constituent materials, but their properties are also determined by the moisture and porosity (Kodur, 2014).

All mechanical and physical properties of concrete are affected by high-temperature exposures. The compressive strength is of principal interest in designing concrete fire-resistant structures. At ambient temperature, the compressive strength of concrete is influenced by the water/cement ratio, curing conditions, type and size of aggregates, types of admixtures, type of stress and the transition zone of the aggregate-paste interface (Mehta & Monteiro, 2017). However, the compressive strength at high temperatures depends on the strength measured at ambient temperature, heating rate, and binders (like silica fume, fly ash, and slag) in the batch mix.

Although the tensile strength is governed by nearly similar factors as compressive strength, concrete is generally proven to be weak in tension. For the normal strength concrete, the

tensile strength is only 10% of its compressive strength and is further reduced for high strength concrete; hence the cracks can easily propagate in concrete under tensile loads. Although the tensile strength of concrete is habitually neglected in calculating the strength at room and high temperatures, the property is crucial in cases where there is a circumstance of fire-induced spalling in concrete structural elements (Rashad, 2015).

#### **2.4 Properties of Concrete containing Neem Seed Husk Ash**

The thermal analysis study done by Musa (2014) on cement paste showed similar thermogravimetric and differential thermal analysis (TGA/DTA) curves for the control (0%) and cement partially substituted with up to 25% of NSHA produced at 600 °C calcination temperature. He observed improvement in strength when 5% of NSHA replaced cement. This gives a justification for the participation NSHA in the hydration progression of the system.

Musa and Ejeh (2012) in another study showed the existence of a synergic effect by NSHA on mortar strength and they recommended its application in the cement-sand mortar. In another study; Ejeh, Abubakar, Ocholi and Nurudeen (2014) experimentally studied the influence of NSHA on strength properties of concrete partially replaced by up to 25% of NSHA. Slump increase was observed at 5% and 10% replacements followed by a decrease in the slump at 15%, 20% and 25% replacements.

In their study, Ibiwoye and Naalla (2017) examined the impact of NSHA on the workability of concrete. Neem seed husk ash substituted cement at 5%, 10%, 15%, 20% and 25% by weight and the workability tests were done for each ratio. The slump values of NSHA concrete decreased from 5.50 mm to 10.00 mm at 0% and 25% respectively.

#### **2.5 Concrete containing Fly Ash at Elevated Temperatures**

Xu, Wong, Poon and Anson (2001) did an investigation on the residual properties of pulverized fly ash (PFA) and they noticed an improvement in compressive strength for exposures after 250 °C, which probably resulted from the hardening due to drying of cement paste and further hydration of cementitious materials. The inclusion of PFA improved the fire resistance as portrayed by a comparatively greater residual compressive strength of PFA concrete over plain concrete when subjected to temperatures of 450 °C and 650 °C.



Potha, Shobha and Rambabu (2004) investigated the influence of heat exposure on flexural strength using M28, M33 and M35 concrete grades with 10%, 20% and 30% of fly ash partially substituting cement. The samples were subjected to 100 °C, 200 °C and 250 °C retained for 1 h, 2 h and 3 h in an electric oven. The concrete specimens containing up to 20% fly ash content performed better than those with no fly ash.

Arioz (2007) studied the physical and mechanical properties of different concrete combinations prepared by OPC, crushed limestone, and river gravel. The loss in weight and compressive strength for the samples exposed to temperature ranges between 200 °C and 1200 °C were determined. The experimental results showed a substantial reduction in the weight of specimens as temperature increased, and it was well-defined further than 800 °C. A relative decrease in concrete's strength was also observed upon increasing the exposure temperature and was more prominent for samples having river gravel aggregate.

Awal and Shehu (2015) presented the experimental results from their study on the functioning behavior of concrete having high volume palm oil fuel ash subjected to extreme temperatures of 200 °C, 400 °C, 600 °C and 800 °C in an electric furnace retained for 1 hour for each targeted ultimate temperature. Higher weight loss, residual compressive strength and the ultrasonic pulse velocity of concrete were observed at higher temperatures. The concrete containing ash performed satisfactorily at high temperatures.

Gar *et al.* (2017) examined the potential application of sugar cane bagasse ash (SCBA) in concrete exposed to maintained elevated temperatures. In their study, the prepared concrete samples were exposed to and through 300 °C, 400 °C and 500 °C and retained for 2 hours in each of the selected temperatures. The residual strength of heated samples was assessed and judged against the non-heated samples in terms of their performance. The findings strongly suggest that the application of SCBA as a pozzolanic admixture imparts high-temperature resistance when used in concrete.

Wang *et al.* (2017) experimented the influence of rice husk ash (RHA) on strength and temperature endurance of concrete. The compressive strength tested at assorted temperatures with different amounts of RHA replacing cement. Rice husk ash was observed to improve strength and temperature resistance by 50% more than the conventional concrete at 800 °C.

Based on the aforementioned facts on the behavior of concrete when exposed to elevated temperatures, this study will focus on assessing the physical properties and the compressive strength of normal concrete strength incorporated with NSHA subjected to and through targeted temperatures.

## **CHAPTER THREE**

### **MATERIALS AND METHODS**

#### **3.1 General Overview**

This chapter provides the detailed properties of the material and the test procedures that were utilized in this study. Tables and figures are provided to better describe the methodology used.

#### **3.2 Materials**

##### **3.2.1 Cement**

The locally available ordinary Portland cement type II (Twiga plus) class 42.5 N conforming to Tanzanian standard TZS727:2002 in accordance with the British standard, BS 12:1996 13 was purchased in the city (Arusha) and was used in this study to attain early strength concrete. Type II cement is produced by obtaining particles that are finer than type I cement. The finer particles provide more surface area thus allowing more hydration to occur on the surfaces. Table 3 illustrates the mineralogical composition of the cement utilized in this study.

Table 3: Chemical composition of cement

Chemical properties	Cement (%)
SiO <sub>2</sub>	17.4
CaO	57.4
Al <sub>2</sub> O <sub>3</sub>	4.9
Fe <sub>2</sub> O <sub>3</sub>	3.0
MgO	0.5
SO <sub>3</sub>	2.7
Loss on Ignition	9.9
Blaine-specific surface area (m <sup>2</sup> /kg)	431
Initial setting time (minutes)	147
Compressive strength 28 days (MPa)	46

### 3.2.2 Coarse Aggregates

Crushed aggregates with the wide-ranging sizes to a maximum of 20 mm were employed as coarse aggregates. They were locally purchased from Kerai Construction Company, operating within the city (Arusha). Figure 2 provides a visual explanation of the aggregates used.



Figure 2: Coarse aggregates

### 3.2.3 Fine Aggregates

The locally accessible natural river sand obtained from within Arusha city was used as fine aggregates with utmost 4.75 mm size. Figure 3 gives a visual explanation of the sand used.



Figure 3: Fine aggregates

### **3.2.4 Water**

Drinking water was used for mixing the concrete. This water contains dissolved solids less than 1000 parts per million.

### **3.2.5 Neem Seed Husk Ash**

The NSHA locally produced in the laboratory was used as the mineral admixture. Figure 4 provides a visual description of the NSHA investigated in this study.



Figure 4: The NSHA used in this study

## **3.3 Experimental Procedures**

### **3.3.1 Preparation of Neem Seed Husk Ash**

The neem seed husks with a moisture content of 1.8% were locally collected from Singida, the central region of Tanzania and were oven-dried at 110 °C for six hours then ground to a small size ranging between 0.07 mm and 10 mm before calcining. The NSHA was obtained by calcining the neem seed husk in an electric furnace at 10 °C/min heating rate to temperatures ranging from 600 °C to 1000 °C as determined by thermogravimetric analysis of neem seed husks. The ashes produced at each temperature are shown in Fig. 5. They were detained for six hours in each of the targeted temperatures followed by grinding and sieving through 125 µm sieve. The heating regimes were adopted from the previous study which

assessed the pozzolanic activity of palm oil waste ash in response to calcination temperatures and retention time (Altwair, Johari & Hashim, 2011).

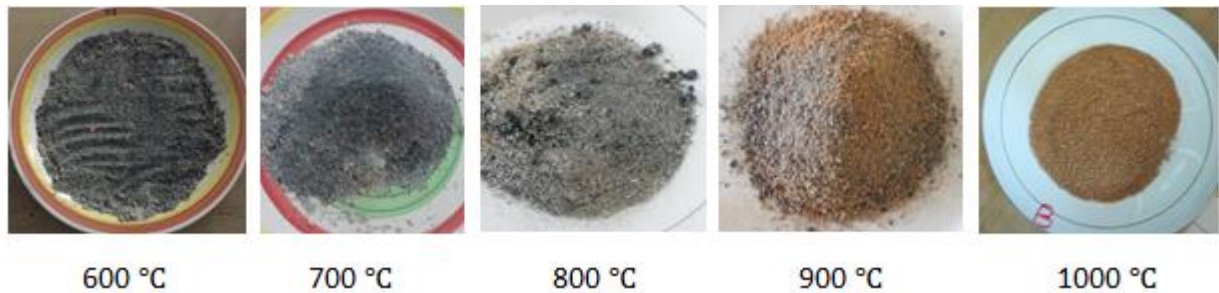


Figure 5: The NSHA produced at different calcination temperatures

### 3.3.2 Characterization of Neem Seem Husk Ash

X-ray fluorescence (XRF) was used to determine the chemical composition of NSHA while the calculation of the specific surface area was done using the Brunauer-Emmett-Teller (BET) method from nitrogen adsorption-desorption studies.

### 3.3.3 Properties of Aggregates

In concrete mix design, some properties of aggregates need to be determined in the first place since they are inputs for having the proportions of ingredients required to produce the desired properties of fresh and hardened concrete's state. The water holding capacity, specific gravity, amount of moisture present, and fineness modulus are essential and were calculated as described below;

#### i. Moisture Content

It is referred to as the extent of water existing within the aggregates expressed as a percentage of the dry mass of aggregates. Such a quantity of water gets accumulated in the pores of aggregates and can easily be removed through drying in an oven with an utmost temperature of 110 °C. Guided by the BS 1377: Part 2: 1990, equation (5) was employed to compute the moisture content;

$$w = \left( \frac{m_2 - m_3}{m_3 - m_1} \right) \times 100\% \quad (5)$$

Whereas  $m_1$  is the measured mass of the container (g);  $m_2$  is the measured mass of the wet soil plus the container (g); and  $m_3$  is the measured mass of the dry soil plus the container (g).

## ii. Water Absorption

This property provides an impression on the core assembly of aggregate. Aggregates with higher absorption values are highly spongy in nature and are mostly deemed unsuitable, except when proven to be satisfactory through testing their strength, resistance to impact loads and hardness. Water absorption ( $w_{ab}$ ) was determined from the laboratory tests and computed equation (6) as per BS 812-2:1995; whereby  $w_1$  is the air measured weight of saturated aggregates (g), and  $w_2$  is the air measured weight of oven dried aggregates (g).

$$w_{ab} = \left( \frac{w_1 - w_2}{w_2} \right) \times 100\% \quad (6)$$

## iii. Specific Gravity

Specific gravity ( $G_s$ ) is expressed as “the ratio of the weight of aggregate to the weight of an equal volume of water”. The  $G_s$  test is usually performed to evaluate their quality of strength properties. In this study, it was determined using the pycnometer and calculated using equation (7) in accordance with ASTM C128-07a.

$$G_s = \frac{W_2 - W_1}{[(W_4 - W_1) - (W_3 - W_2)]} \quad (7)$$

Where;  $W_1$  is the weight of pycnometer in the air (g),  $W_2$  is the weight of aggregates and pycnometer (g),  $W_3$  is the weight of aggregates, pycnometer, and water (g) and  $W_4$  is the weight of water and pycnometer in the air (g).

## iv. Sieve Analysis

The particle size distributions for both the fine and coarse aggregates were obtained through sieving the aggregates using sieves specified in Table 2. The following procedures were adopted;

- a. The representative samples of aggregates were oven-dried at 110 °C.



- b. A set of selected sieves were arranged to start with the largest sieve size and then air-cooled samples were sieved through.
- c. The sieves were shaken individually over a clean tray for about three minutes until no further particles went through. The sieves were shaken in frequently varying directions and motions to ensure a constant movement of materials over the sieve.
- d. Blocks of fine materials were fragmented by light pressure using fingers against the sieve sides. The openings in the sieve underside were freed up using a soft brush.
- e. The materials retained per sieve including those cleaned from the mesh were weighed after a complete sieving process.

The sieve analysis results were then utilized to calculate the fineness modulus as per the equation (4) described in the previous chapter.

#### **3.3.4 Mix Design Methods for Concrete**

The proportioning and the mixing of concrete ingredients were done as per BS 1881 - 125:1986 (BSI, 1986) for all concrete series. The process involved the essential steps which are highlighted as follows:

- i. The target mean strength was estimated as a function of the specified characteristic strength based on the required quality control level.
- ii. The water/cement ratio was chosen as a function of the estimated target mean strength and examined for the required durability.
- iii. Selecting the content of water for the expected workability.
- iv. From the selected water/cement ratio and the determined water content, the content of cement content was then determined and checked for the water requirements.
- v. Percentages of coarse and fine aggregates were relatively selected based on their determined properties.
- vi. Determination of the proportions of the trial mix.

- vii. The compressive strength from the trial mix was tested and appropriate modifications were made to attain the ultimate mix composition.

### 3.3.5 Concrete Mix Proportions

The targeted concrete strength used was 25 MPa for the 28 days of curing, and the slump of 60 – 180 mm was used. The maximum nominal size of aggregate selected was 20 mm. The measured properties of aggregates presented in Table 5 were employed to obtain the mix proportions for the concrete materials. Earlier studies suggest that up to 10% replacement of cement by NSHA offers the optimum performance (Musa, 2013; Ejeh, Abubakar, Ocholi & Nurudeen, 2014; Raheem & Ibiwoye, 2018). The blended concrete mixes used in this study were prepared by substituting cement contents by various percentages of NSHA. The descriptions of the assorted mix proportions used are summarized in Table 4. The ratios of the concrete ingredients (cement: fine aggregates: coarse aggregates) based on the quantities obtained through the concrete mix design process can now be presented as 1:1.3:3. The detailed procedures for obtaining the mix proportions as per BS 8110 are illustrated in Appendix 5.

Table 4: The designed concrete mix proportions

Components (kg/m <sup>3</sup> )	Percent of OPC replacement (wt. %)				
	0	3	5	7	10
Cement	410	397.7	389.5	381.3	369
NSHA	0	12.3	20.5	28.7	41
Sand	530	530	530	530	530
Aggregates	1260	1260	1260	1260	1260
Water	205	205	205	205	205

### 3.3.6 Production of Concrete

Guided by the British standard of concrete mixing (BSI, 1986), the concrete blends were prepared using an electric concrete mixer as displayed in Fig. 6. The weighed aggregates (fine and coarse) were put into the concrete mixer and moisturized in advance before adding water to their saturation. Afterward, water was added with the addition of cement together with the NSHA and thoroughly mixed for 3 minutes. Concrete was prepared by partially

substituting cement by NSHA. Five series of test specimen were considered in this research; one series of specimens of normal strength concrete (with 0% NSHA) and four series of specimens of cement-NSHA concrete with replacements of cement by 3%, 5%, 7% and 10% NSHA. The produced fresh concrete was then tested for workability before casting.



Figure 6: Concrete production

### **3.3.7 Workability of Concrete**

Workability is the property that defines the easiness and homogeneity by which freshly mixed concrete or mortar can be transported, cast, compacted, and finished. The desired final properties of concrete in the hardened state are very much dependent on the workability of the fresh concrete. It also affects the labor costs in placing and compacting. Basing on the flow type produced by concrete during the test, test methods for workability are commonly classified as the Slump Test, Compacting Factor Test, Vee Bee Consistometer Test, and Flow Table Test. The slump method test was utilized to ascertain the empirical values of the workability of concrete produced in this study. The test is common due to the easiness in using the apparatus and the procedures are simple to follow. The apparatus comprises of slump cone, a measurement scale and a rod for tamping. The height of the cone is 300 mm with diameters measured as 200 mm and 100 mm for the base and top openings respectively.

The fundamental steps applied in testing for slump as stipulated by BIS: 1199-1959 are:

- i. The apparatus were washed before carrying out the test to reduce the friction of concrete against their surfaces.

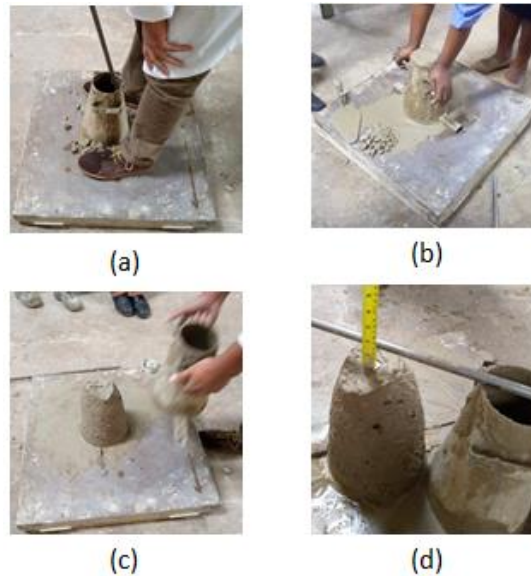


Figure 7: Slump testing: (a) temping (b) surface leveling (c) slumping (d) slump measurement

- ii. The cone's base was rested on a flat surface and then filled with concrete in approximately three equal layers before testing for its workability.
- iii. Every concrete layer was temped 25 times using a 16 mm standard diameter steel rod with a curvy end as visually described in Fig. 7(a).
- iv. The upper surface of the filled mold was then leveled through rolling the trowel as shown in Fig. 7(b).
- v. Throughout the whole process, the mold was steadily restrained against its base through its handles and brazed foot - rests over the mold to ensure that no movement due to the pouring of concrete.
- vi. Instantly after leveling the filled concrete, the cone was gently and carefully lifted perpendicularly, the unsupported concrete was then allowed to fall as illustrated in Fig. 7(c).

- vii. The slump is the decreased central height measured from the slumped concrete as referred to the mold's height.
- viii. The slump value was then measured by laying the scale just beside the slumped concrete as shown in Fig. 7(d).

### 3.3.8 Preparation of Concrete Specimens

Standard concrete cubes with a size of 150 mm were used. One hundred and fifty cubes were cast from which three cubes in each series were subjected to each of the selected temperature exposures. The cast specimens were left under room temperature of  $25 \pm 3$  °C to set. After 24 hours, the concrete specimens were demolded and then cured by submerging in water under identical temperature conditions. For the targeted ages (7 and 28 days), the samples were removed from the water and exposed for 24 hours to naturally dry under laboratory environmental conditions before beginning the process of subjecting them to higher temperature treatment. Figure 8 provides a pictorial description of the concrete samples preparation process.

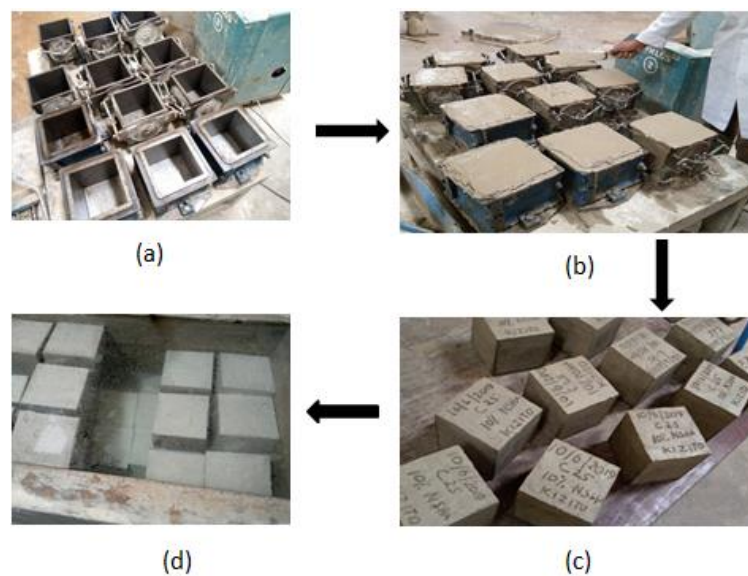


Figure 8: Sample preparation: (a) molds; (b) casting; (c) demolding; and (d) curing

### 3.3.9 Thermal Treatment

The cured concrete samples were subjected to a range of controlled temperatures using thermostat electric furnace to the chosen different levels of temperature (200 °C, 400 °C, 600 °C and 800 °C). The temperature was set to gradually rise at 10 °C/min, a methodology

similar to an earlier study (Chen *et al.*, 2009), and the samples retained for a period of 3 hours in each target temperature as shown in Fig. 9(a). To avoid cracking due to temperature gradient, the heated cubes were cooled with a constant natural rate of fall of temperature within the furnace to room temperature. The cooled samples as in Fig. 9(b) were then considered for residual strength testing.

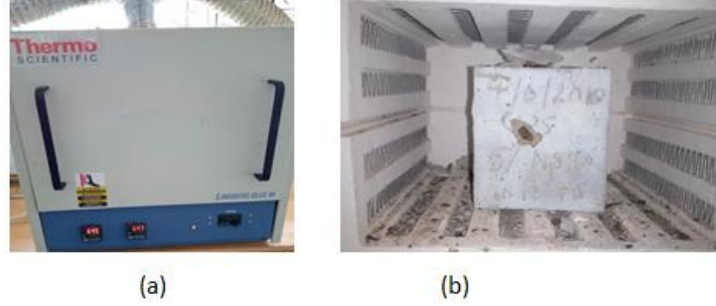


Figure 9: Thermal treatment for concrete cubes: (a) heating, and (b) cooled sample

### 3.3.10 Testing Program

The mass loss of concrete was assessed by weighing digitally the samples by means of electronic balance which is  $\pm 0.1$  g accurate. All specimens other than the control samples were weighed before firing ( $M_{initial}$ ) and the control samples were tested with no heat application. After cooling, samples were reweighed ( $M_{heated}$ ) and assessed for any spalling resulting from thermal treatment. The measured weights were then employed in determining the overall mass loss ( $M_{loss}$ ) at each temperature using equation (8) (Owaid *et al.*, 2016).

$$M_{loss} = \frac{M_{initial} - M_{heated}}{M_{initial}} \quad (8)$$

Their residual compressive strength was then determined using the compressive strength testing machine with a full load capability of 3000 kN with a loading scale of 5 kN for every division as demonstrated in Fig. 10. The concrete samples were compressively crushed at a 100 kN/min loading rate. The crushing loads were obtained by loading the samples to failure as described by BS EN 12390-3 (BSI, 2009).



Figure 10: Compressive strength testing machine

The compressive strength ( $f_c$ ) was computed as the function of the crushing load,  $F$  (N) and the cross-section area of the concrete cubes,  $A$  (mm<sup>2</sup>) using the equation (9). The reported ultimate compressive strengths were calculated as the average of the three individual cubes in each series considered.

$$f_c = \frac{F}{A} \quad (9)$$

## CHAPTER FOUR

### RESULTS AND DISCUSSION

#### 4.1 Properties of Aggregates

The necessary properties of aggregates were determined in the laboratory as per BS 882:1992 (EN, 1992) as described in Appendices 2, 3 and 4. The determined properties are inputs in the concrete mix designing process. Table 5 portrays the measured properties of aggregates that were used in this experimental study.

Table 5: Measured properties of aggregates

Properties	Coarse aggregates	Fine aggregates
Water absorption (%)	1.65	1.89
Specific gravity	3.12	2.77
Bulk density (kg/m <sup>3</sup> )	1465	1590
Moisture content (%)	3.48	4.99
Fineness modulus	3.18	2.16

Due to its importance in concrete strength, the specific gravity of aggregates ranging from about 2.5 to 3.0 is recommended (Neville & Brooks, 2010). Materials with higher values of specific gravity are generally believed to have higher strength. The specific gravity of 3.12 and 2.77 for coarse and fine aggregates respectively used in this study agree with the requirement and hence are suitable for concrete production. The amount of water held in aggregates provides an indication of the porosity level. Water absorption measures aggregates' ability to resist weathering and frost actions. Moisture content determines the amount of water accumulated in the pores of aggregate. In concrete production, moisture content gives an amount to be reduced whereas the water absorption value gives the extent of additional water needed.

Grading of the used aggregates was done by sieving through a set of sieves described in Table 2. The distribution of particle sizes of the used aggregates is shown in Fig. 11. The well-graded curves obtained indicate that the aggregates meet the criteria for their use in concrete production as it was afore-described.



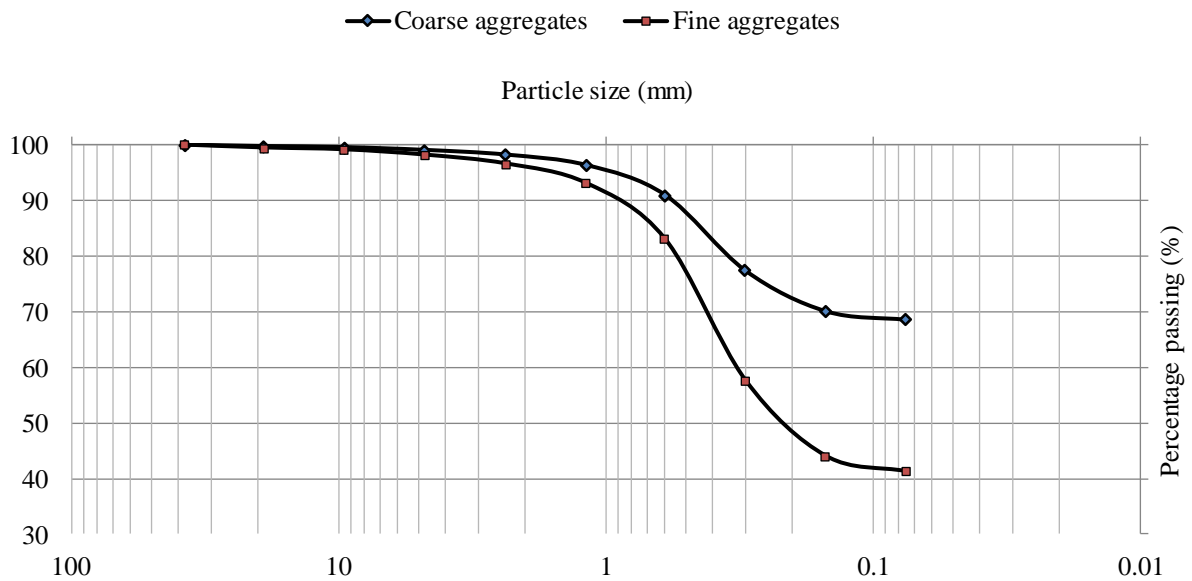


Figure 11: Particle size distribution of the used aggregates

## 4.2 Production of Neem Seed Husk Ash

The NSHA was produced in the laboratory from the neem seed husks. Preliminary analysis to select suitable calcination temperatures was done followed by the characterization of the ashes to assess their suitability as supplementary cementitious materials (SCMs).

### 4.2.1 Thermogravimetric Analysis

The thermogravimetric analysis (TGA) of neem seed husks provides the basis for the decision of calcination temperatures to be considered. From Fig. 12 it is evident that calcining the neem seed husks beyond 500 °C may result in decomposition of organic contents to a large extent thereby yielding metallic oxides which can be considered as essential additives in concrete production. The previous study by Adebisi *et al.* (2019) also recommended that the calcination temperature of greater than 500 °C is suitable to extract silica from Maize Stalk, Sugarcane Bagasse, and Cassava Periderm. Such an observation agrees with the findings of the current study.

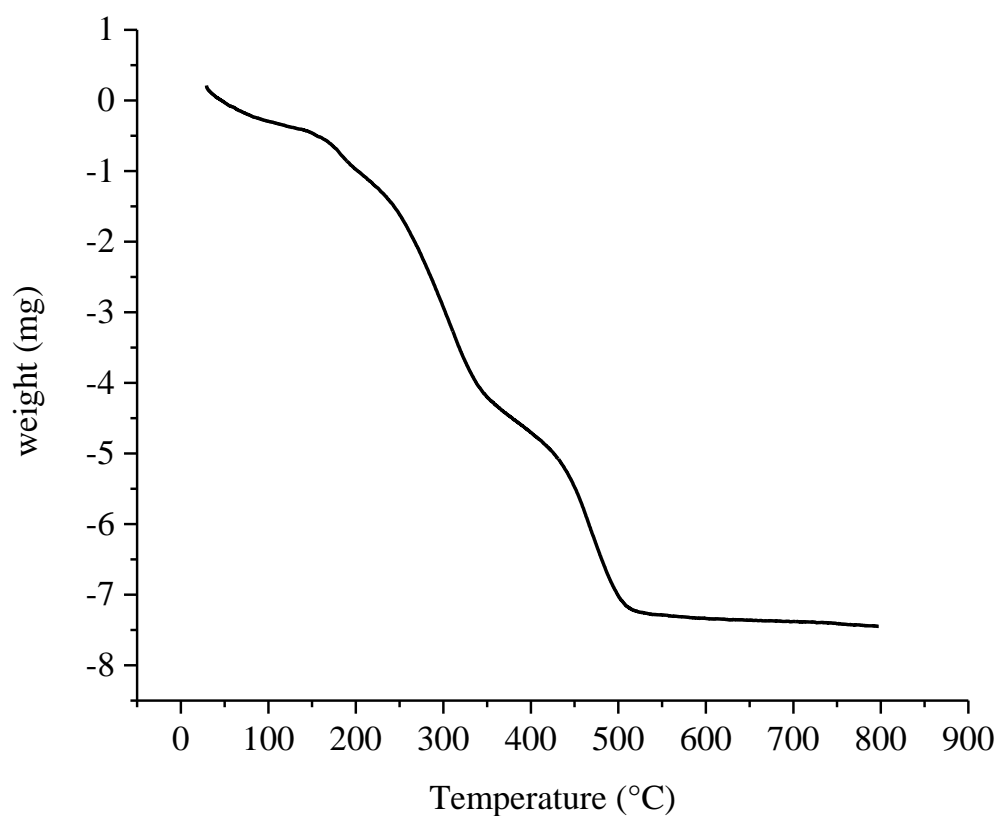


Figure 12: The TGA curve for the neem seed husks

#### 4.2.2 Characterization of Neem Seed Husk Ash

The X-ray fluorescence (XRF) and BET characterizations were done on NSHA samples, and the results are displayed in Table 6. The elemental compositions and the specific surface area are studied as the function of calcination temperatures.

Table 6: XRF and BET results

Sample Name	NSHA-600	NSHA-700	NSHA-800	NSHA-900	NSHA-1000
SiO <sub>2</sub> (%)	33.53	34.1	45.23	41.74	37.46
Al <sub>2</sub> O <sub>3</sub> (%)	20.47	21.59	22.59	21.05	21.89
Fe <sub>2</sub> O <sub>3</sub> (%)	2.41	2.29	3.4	2.31	2.42
CaO (%)	2.58	2.65	2.56	2.38	2.96
MgO (%)	3.00	2.95	3.32	2.57	3.11
K <sub>2</sub> O (%)	2.71	2.35	2.73	1.95	2.68
Na <sub>2</sub> O (%)	0.23	0.24	0.22	0.26	0.26
SO <sub>3</sub> (%)	0.76	0.65	0.84	0.48	0.64
Cl (%)	0.18	0.09	0.16	0.03	0.09
LoI (%)	5.30	5.30	5.63	4.67	5.72
(SiO <sub>2</sub> + Al <sub>2</sub> O <sub>3</sub> + Fe <sub>2</sub> O <sub>3</sub> )%	56.41	57.98	71.22	65.1	61.77
Blaine-Surface Area (m <sup>2</sup> /kg)	490	410	544	216	352

For the neem seed husks considered in this investigation, calcination temperatures ranging from 600 °C – 1000 °C were studied against the properties of the produced ashes. The pozzolanic activity is determined largely by the aluminosilicate content in the material, that is, (SiO<sub>2</sub> + Al<sub>2</sub>O<sub>3</sub> + Fe<sub>2</sub>O<sub>3</sub>)%. From the results, NSHA-800 has shown a larger pozzolanic activity value (71.2%) and is categorized as class F fly ash which is suitable for applications as pozzolanic materials in concrete. The pozzolanic activity was observed to decrease for calcination temperature beyond 800 °C, such a decrease may be due to crystallization of the SiO<sub>2</sub> and development of cristobalite similar to the observation by Soares *et al.* (2014). The surface area also decreases for higher calcination temperatures (above 800 °C) which might be initiated by the agglomeration of the NSHA particles. The extreme acceptable loss on ignition for class F and C fly ash specified by ASTM C618 is 6%. The loss on ignition for NSHA produced is less than 6%, clearly meeting the requirement specified by ASTM C618.

### 4.2.3 Gradation of Neem Seed Husk Ash

The reactivity of fly ash, when employed as partial substitution of cement in concrete mixes, depends to a large extent on chemical composition and the particle size distribution. The fraction of ashes passing the  $45\ \mu\text{m}$  sieve is suitable for application in concrete production as the reactivity of fly ash proportionally increases with its fineness (Butler & Kanare, 1988). Basing on the particle size distribution of the NSHA presented in Fig. 13, a large portion (80%) of the used NSHA have less than  $45\ \mu\text{m}$  particle size. The improved strength is highly expected as a result of the reactivity of the NSHA when partially substitutes OPC in concrete.

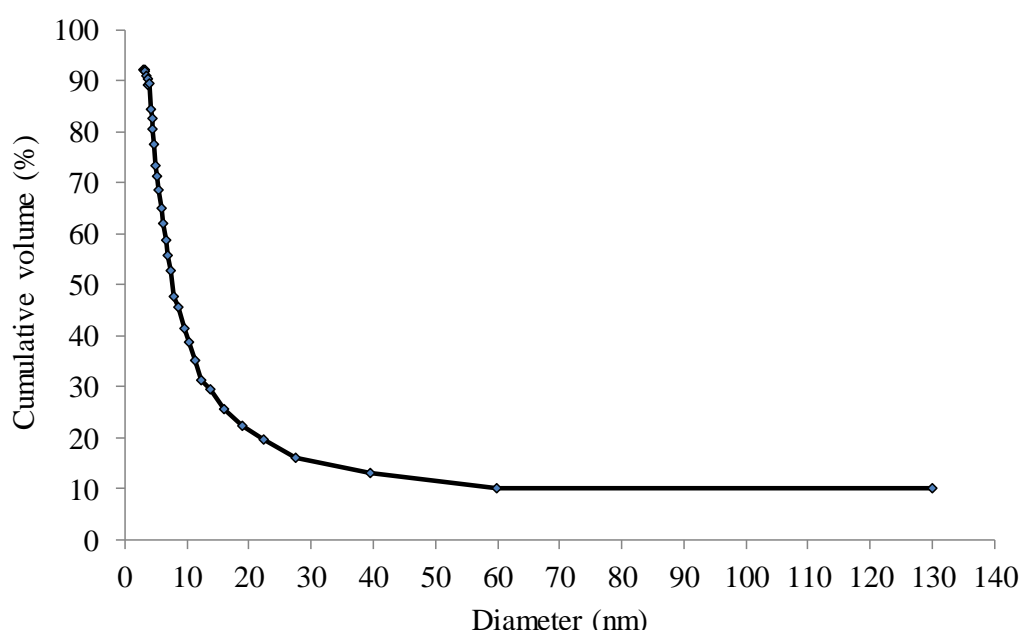


Figure 13: Particle size distribution of NSHA

### 4.3 Properties of Fresh Concrete

The workability of the produced concrete in each of the series was tested by the slump apparatus. The slump values in each batch and the standard deviations of the test results are presented in Fig. 14. The values of slump decrease with the addition of NSHA; this implies that NSHA is highly hygroscopic materials and results in the stiff concrete mixture when a large amount is utilized. The observed workability in this study agrees with the findings by Ibiwoye and Naalla (2017) and Fang, Ho, Tu and Zhang (2018). The increasing concentration of silica upon adding the NSHA in the concrete is what raises the water demand to produce a workable concrete (Adesanya & Raheem, 2009).

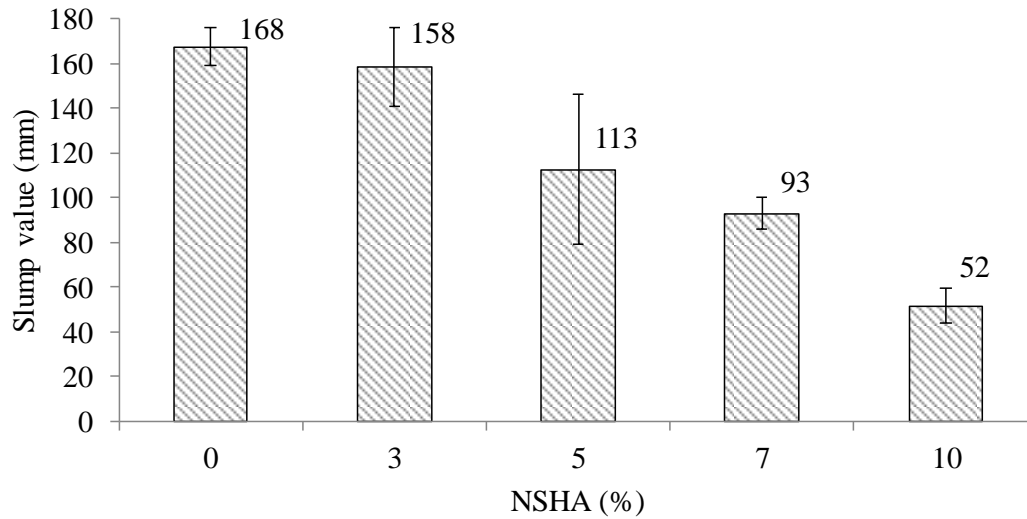


Figure 14: Slump values for all concrete batches





















#### 4.4 Properties of Hardened Concrete

##### 4.4.1 Physical Characteristics with Temperature Rise

The evaluation of impairment to the concrete structures subjected to extraordinary temperatures was thoroughly done to observe the changes occurring to the surface of concrete specimens. Visual observation of color changes, spalling and surface cracks on concrete is considered to be the first step in assessing the damages of fired concrete. Visual observation of fired concrete which was considered as the first step assessment discovered a similar pattern of cracks and pits on the surfaces of both the 7 and 28 days cured concrete samples. The physical appearances of concrete at various temperatures of exposure up to 800 °C are presented in Table 7. For all ratios of concrete, the surfaces showed no significant change when subjected to temperatures up to 400 °C while having the same appearance and color. At a temperature of 600 °C cracking and spalling were observed and they became widely noticeable at 800 °C. The spalling behavior is associated with the generated pore pressures and growth of cracks, which in turn are affected by the heating rate and the composition of the heterogeneous concrete. A similar observation was observed in previous works (Owaid *et al.*, 2016). This suggests that the maximum safe temperature of 400 °C can be attained when NSHA admixtures are incorporated in concrete, though the behavior of concrete at temperatures ranging between 400 °C and 600 °C might be considered for future works to be sure of the threshold temperature.

Though the spalling occurs both on normal and blended concrete, the effect is severe in concrete containing the NSHA. The surface cracking and breaking as characterized by holes is observed to increase with the increasing percentages of NSHA in the blended concrete samples. This is due to higher internal pore pressure which develops as a result of temperature rise. The addition of NSHA in concrete results in a less permeable concrete that prevents free escaping of vapor from the inner part, which escapes by exploding leaving behind the holes on the surface (Kodur, 2014).

Table 7: Physical characteristics of concrete mixes at elevated temperatures

Mix	200 °C.	400 °C.	600 °C.	800 °C.
0% NSHA				
3% NSHA				
5% NSHA				
7% NSHA				
10% NSHA				

#### 4.4.2 Spalling and Mass Loss

Figure 15 displays the concrete mass loss in relation to the initial weight of the samples of OPC and cement-NSHA blended concrete properly cured for 7 days with increasing exposure temperature. It is clearly seen that non-NSHA concrete samples studied revealed a gradual increase in mass loss from 10.7% to 15.3% for the temperature increasing from 200 °C to 800 °C. The NSHA concrete samples displayed a small loss in mass in comparison to the control mix (concrete samples with no NSHA) ranging from 4.8% to 10.0% for the temperature increasing from 200 °C to 800 °C. The experimental findings also indicate a decrease in a mass loss upon increasing the NSHA materials. Such a decrease in a mass loss might be attributed by the dense matrices of the NSHA concrete as compared to the mix which does not contain NSHA as the mass loss is caused by air voids associated with the loss of free and chemically bound water from the paste. Similar findings were previously reported (Janotka & Nürnbergerová, 2005; Owaid *et al.*, 2016). Greater mass losses were observed for all batches considered at a temperature of 800 °C which may be attributed by the evaporation of total absorbed and adsorbed water from concrete as it was also observed by Ramesh, Raju and Rekha (2016).

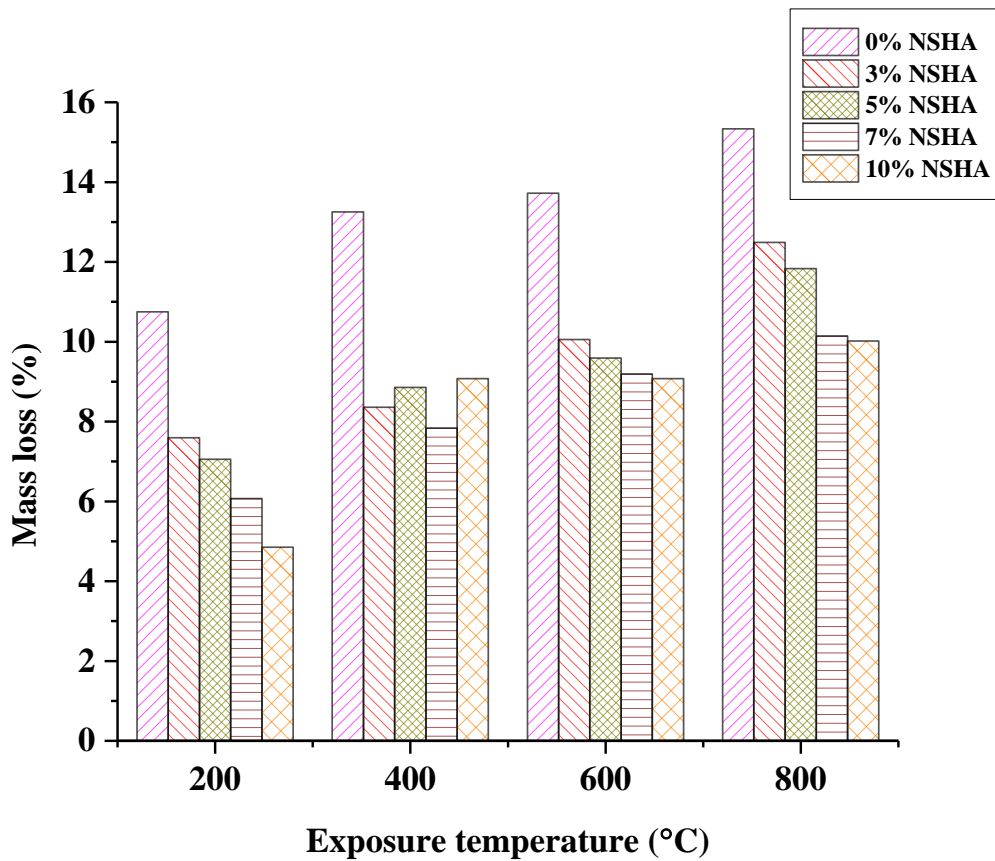


Figure 15: Mass loss versus temperature for OPC and NSHA concrete cured for 7 days

The mass losses for the 28 days cured concrete samples are shown in Fig. 16. A slight similarity in weight loss trend is observed upon increasing temperature as it was observed for the 7 cured samples. In this case, the mass loss for the OPC concrete samples is gradually increased from 8.2% to 12.6% for the temperature increasing from 200 °C to 800 °C respectively. Upon increasing the exposure temperature, it directly increases the mass loss due to releasing of free water and the bound water-related to  $\text{Ca}(\text{OH})_2$  decomposition and the other hydrated cement products developed during the hydration process. A previous study by Janotka and Nürnbergerová (2005) observed similar results. The mass loss at temperatures above 400 °C was associated with disintegration leaving some holes on the surface due to spalling. The results show that mass loss is higher for the early age concrete samples than for the mature concrete samples. For all samples, higher rates of mass loss were observed for temperatures extending from 200 °C to 400 °C, the mass loss slightly increased at 600 °C and 800 °C. The current findings concur with the observations of the earlier study by Fares, Noumowe and Remond (2009), who testified that nearly 70% of the free and bound water evaporates upon exposing the concrete to 300 °C.



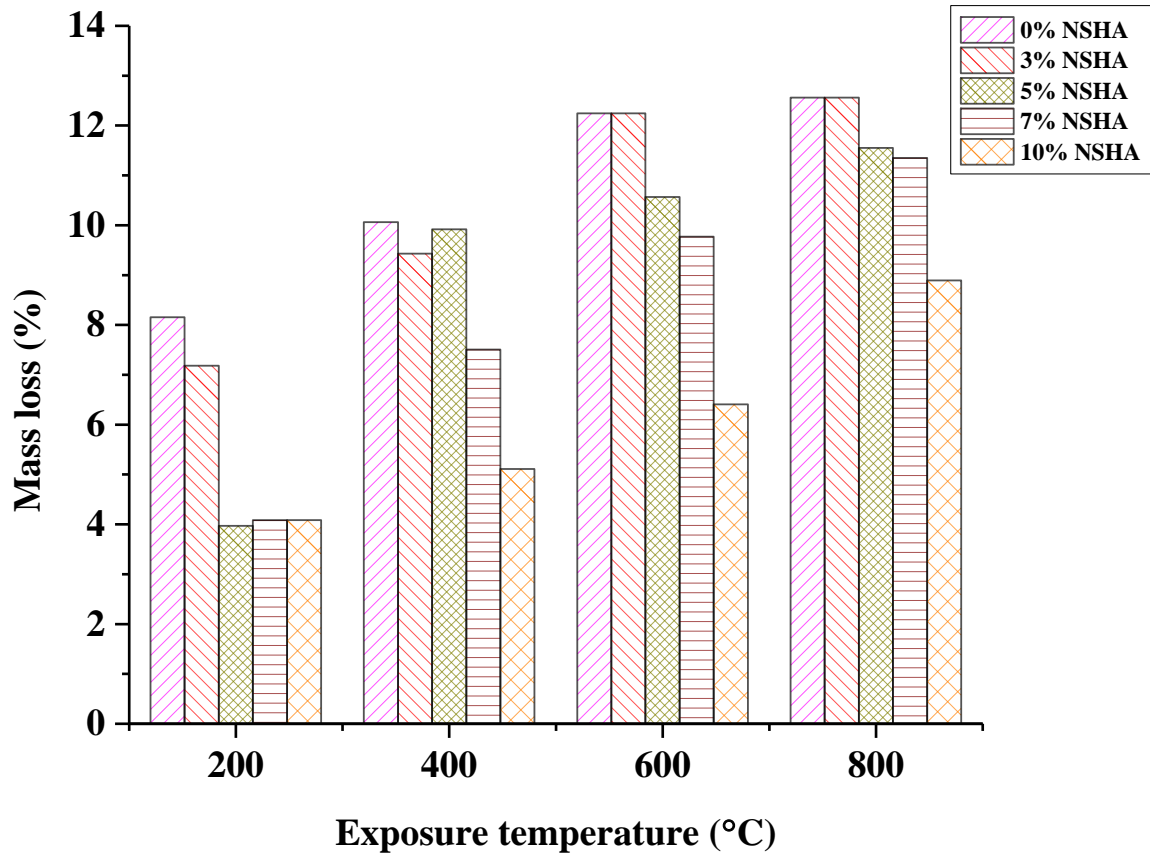


Figure 16: Mass loss versus temperature for OPC and NSHA concrete cured for 28 days

#### 4.4.3 Residual Compressive Strength

The residual strength for the 7 and 28 days cured concrete samples are given in Table 8. The experimental results illustrate a small decrease in compressive strength for temperature rising up to 200 °C; due to the weakening of bonds likely to be ascribed by swelling of water layers in the NSHA-cement paste. However, at a temperature of 400 °C, the strength increased for all samples as a result of extra C-S-H phases yielded from the pozzolanic reaction of NSHA with free lime that gets deposited in the pore system (for concrete containing 3%, 5%, 7% and 10% NSHA) and the internal autoclaving where un-hydrated cement grains undergo further hydration (for the control concrete samples, with 0% NSHA) are responsible for the compressive strength rise as exposure temperature is raised. These observations agree with the findings of the previous studies (Savva *et al.*, 2005; Morsy *et al.*, 2010; Aslani & Bastami, 2011).

Table 8: Residual compressive strength for the 7 and 28 days cured concrete samples

Exposure temperature (°C)	Compressive strength (MPa)									
	0% NSHA		3% NSHA		5% NSHA		7% NSHA		10% NSHA	
	7 d	28 d	7 d	28 d	7 d	28 d	7 d	28 d	7 d	28 d
25	19.7	26.8	20.9	29.4	24.3	30.8	20.0	30.7	20.0	27.3
200	19.1	24.1	24.4	25.0	26.8	29.3	24.5	29.3	23.1	24.5
400	23.2	27.7	24.0	28.4	30.1	33.2	25.8	29.0	24.0	24.7
600	9.7	22.1	15.7	20.9	20.4	24.1	17.0	23.5	15.0	20.3
800	7.3	8.7	8.1	7.0	7.9	8.2	6.7	8.1	9.0	8.3

Figure 17 illustrates the relationship between the compressive strength of assorted cement pastes after 7 days of curing and temperature for which the concrete samples were exposed; the error bars are the standard deviations of the test results. For all batches of concrete, samples considered were observed to maintain their structural integrity for the temperatures ranging from 200 °C – 400 °C while the sample with the optimal replacement of 5% NSHA still performed better up to 600 °C. In the prior investigation, the compressive strength increased at 250 °C and had higher residual strength at 450 °C and 650 °C (Xu *et al.*, 2001; Noumowe, 2005).

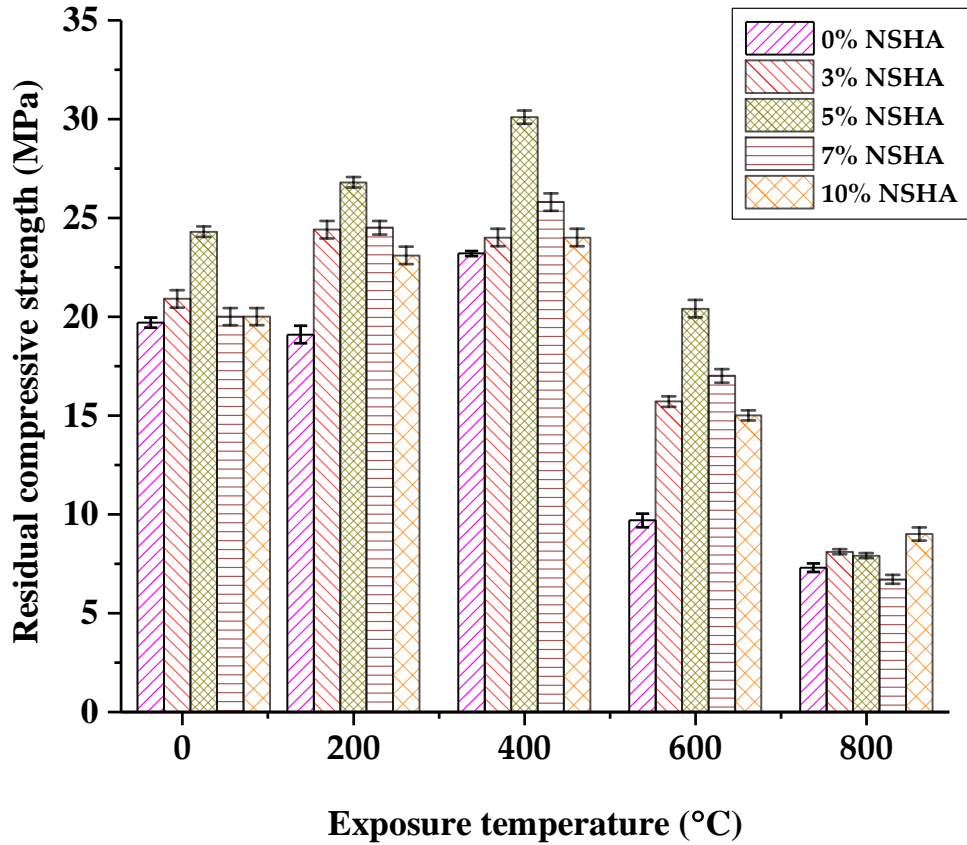


Figure 17: Residual compressive strength versus temperature for the 7 days cured concrete

The outstanding and reduced compressive strength for the heated concrete samples after 7 days curing period is demonstrated in Fig. 18. Incorporating the optimum amount of NSHA gradually raised the residual compressive strength more than for the mix with no NSHA. This is likely to be caused by the pozzolanic reaction of NSHA during the hydration process resulting in the production of a high amount of C-S-H which is accountable for strength development. According to the previous study (Ishak *et al.*, 2019), strength improved at 200 °C due to the hydrothermal interaction of the silica from the NSHA as an outcome of temperature rise with the produced free lime during hydration reaction. The strength started decreasing at 400 °C, 600 °C and 800 °C levels of temperature exposure, such a decrease is likely to be caused by the generated thermal stress around the pores which produce micro-cracks (Wang *et al.*, 2017). The concrete's early age residual strength in the current study was witnessed to be superior to the control mixes by 22.6% and 12.4% at 200 °C and 400 °C respectively followed by noticeable strength drop of 32.2% and 61.2% at 600 °C and 800 °C respectively for the optimal replacement. Moreover, while the application of rice husk ash as

investigated by Wang *et al.* (2017) retained up to 50% of strength at 800 °C, the current study observed about 39% of strength is retained.

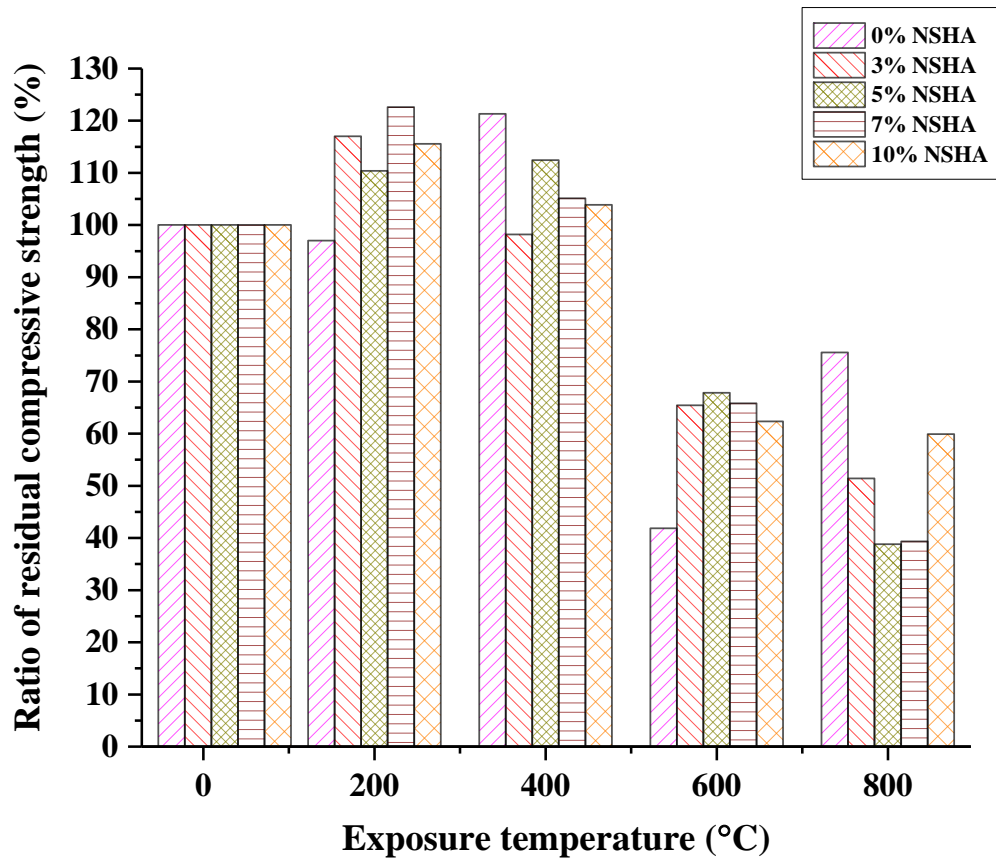


Figure 18: The ratio of residual compressive strength for the 7 days cured concrete

The residual strength for the 28 cured samples with their respective standard deviations is presented in Fig. 19. Like the 7 days cured samples, the concrete samples cured for 28 days showed a similar pattern for samples with 3%, 5% and 7% NSHA. The cement-NSHA blended concrete had a better performance than the control mix to high temperatures up to 400 °C followed by a significant strength reduction. The better performance is caused by the high amount of C-S-H produced by the pozzolanic effect of NSHA with the hydration product resulting in improved strength. The strength reduction at temperatures above 400 °C is caused by the internal pore pressure which results in micro and macro cracks of the compact blended mixes (Wang *et al.*, 2017).

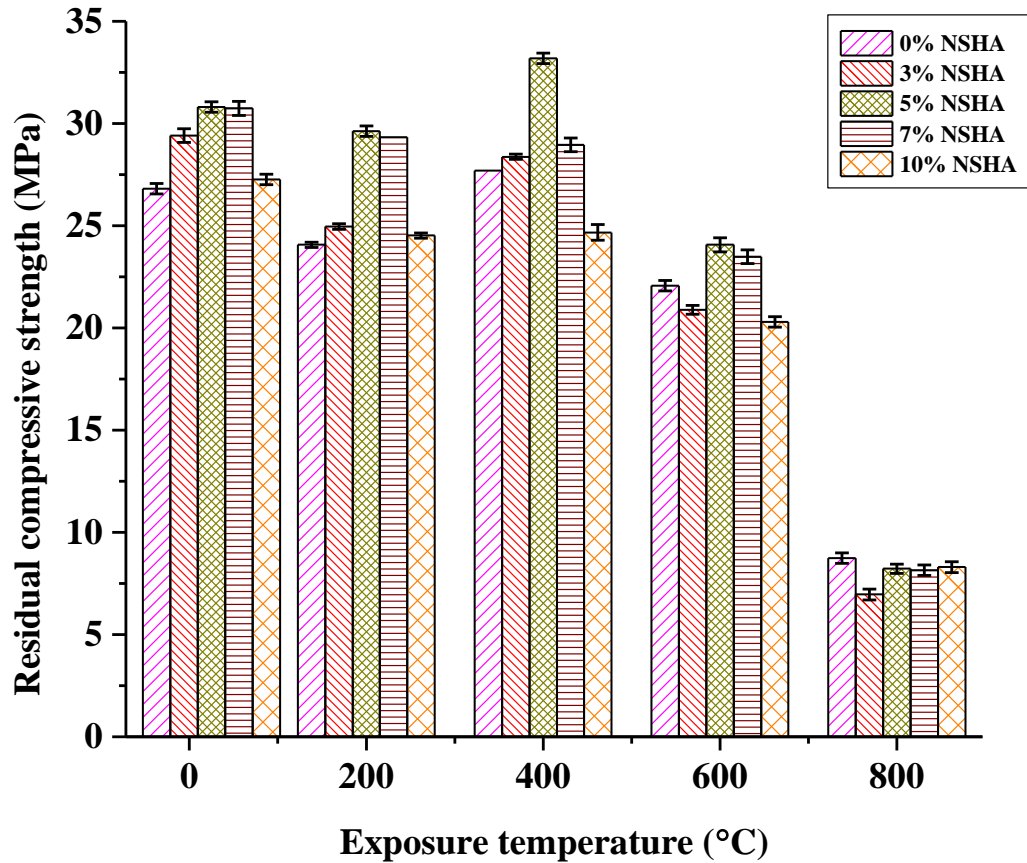


Figure 19: Residual compressive strength versus temperature for the 28 days cured concrete

Figure 20 shows the residual and decreased compressive strength for the 28 cured concrete samples. The residual compressive strength of 5% NSHA concrete is 10.5% and 23.8% greater than 0% NSHA concrete at 200 °C and 400 °C, and then it fell by 10.2% and 69.3% at 600 °C and 800 °C respectively. Both NSHA and non-NSHA specimens display a drastic strength decrease at 600 °C. However, the NSHA contained specimens have a higher residual compressive strength than the non-NSHA contained specimens. The higher strength of NSHA contained samples after subjection to high temperature is likely to be caused by a high amount of C-S-H produced by the pozzolanic effect of NSHA with the hydration product resulting in improved strength. Additionally, NSHA acts like a micro filler that strengthens the microstructure of the system (Horszczaruk *et al.*, 2017).

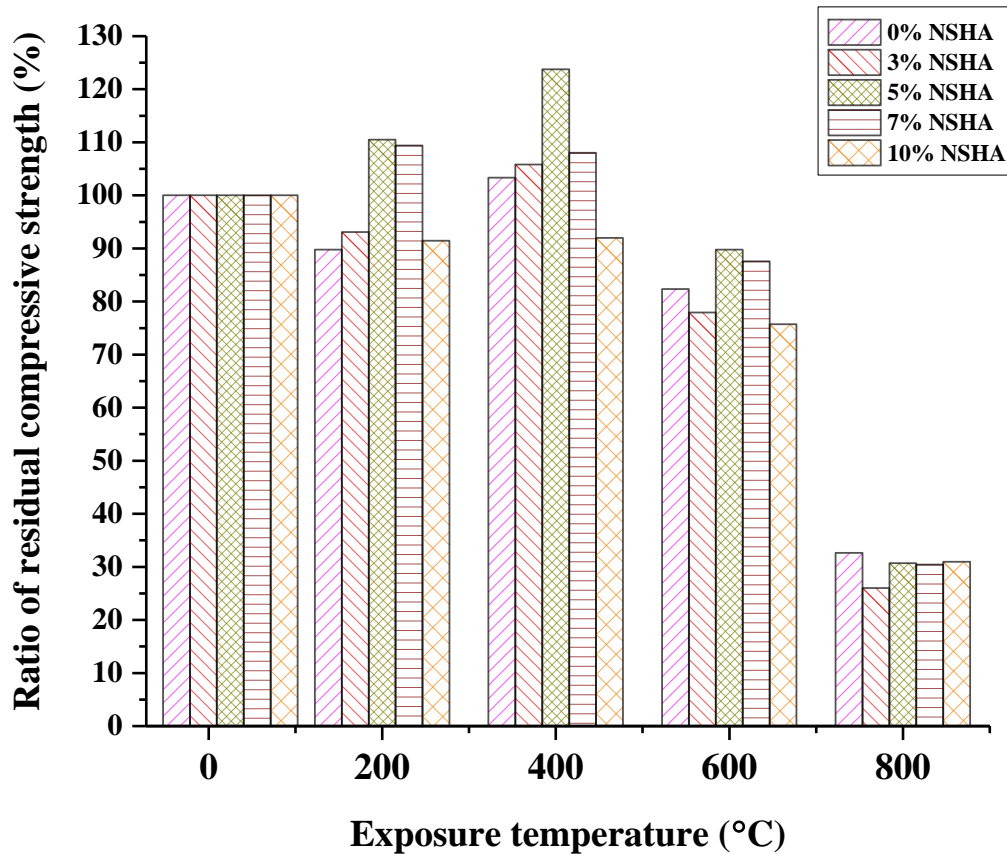


Figure 20: The ratio of residual compressive strength for the 28 days cured concrete

The observed early decrease of compressive strength of concrete samples between 25 °C and 200 °C is due to the weakening of bonds likely to be ascribed by swelling of water layers in the NSHA-cement paste (Morsy *et al.*, 2010). The extra C-S-H phases yielded from the pozzolanic reaction of NSHA with free lime that gets deposited in the pore system and the internal autoclaving where un-hydrated cement grains undergo further hydration are responsible for the compressive strength rise as exposure temperature is raised. Undoubtedly, the results provide evidence that the partial substitution of OPC by 5% of NSHA escalates the compressive strength of cement concrete by about 24% higher than conventional control samples at 400 °C. Hence, the optimal replacement of cement by the synthetic pozzolanic material (5% NSHA) improves the cement paste's capacity to resist fire up to 400 °C.

Conclusively, the general reduction in strength of NSHA concrete is initiated by the compact microstructure, which caused the build-up of high internal pressure resulting from the water-vapor transition in the water interlayer. For temperatures ranging from 400 °C to 600 °C, a severe loss in strength was observed for all concrete batches and recorded as 17.7%, 22.1%,

10.2%, 12.4% and 24.6% of the original values for OPC, 0% NSHA, 3% NSHA, 5% NSHA, 7% NSHA and 10% NSHA concretes, respectively.

The cement paste contracts and the aggregates expand upon exposing the concrete to high temperatures. Such a response leads to the weakening of the transition zone and bonding between aggregates and cement paste; this process, as well as the decomposition of the chemically formed hydration products, results in serious deterioration and strength loss in concrete exposed to elevated temperatures. An average strength loss of 70% was observed for concrete containing NSHA which deteriorated severely up to 800 °C due to the decomposition of C-S-H gel. Such an observation has been testified in previous studies (Morsy *et al.*, 2010; Owaid *et al.*, 2016). Despite the improved early strength of concrete containing NSHA, a noticeable loss in compressive strength was witnessed at high temperatures as a result of built-up vapor pressure in a dense structure during the evaporation process of the physically and chemically bound water.

## CHAPTER FIVE

### CONCLUSION AND RECOMMENDATIONS

#### 5.1 Conclusion

The present study examined the residual compressive strength and spalling effect of the cement-NSHA blended normal concrete (with characteristic strength of 25 MPa) subjected to elevated temperatures. The mixes containing 5% NSHA exhibited greater compressive strength (33.2 MPa) than the control mix (26.7 MPa), implying that the inclusion of NSHA led to improved compressive strength both at ordinary and elevated temperatures. The blended concrete was found to perform better than the normal concrete when fired up to 400 °C. The strength decreased significantly for concrete specimens fired beyond 400 °C associated with higher mass losses due to spalling. Several deductions can be made grounded on the presented experimental results as follows:

- i. Calcination temperature of 800 °C produced the NSHA with higher pozzolanic activity and surface area. The current study recommends it as the optimum temperature for the production of NSHA from the neem seed husks.
- ii. For all concrete samples exposed up to 400 °C, there was no noticeable consequence on the surface. Significant fractures and localized spalling were noticed when the exposure temperature rose to 600 °C and they were more pronounced at 800 °C. The color change was insignificant for all series of OPC and blended concrete considered.
- iii. Specimens exposed to temperatures beyond 400 °C suffered a spalling and severe mass loss. From the previous findings by Bastami, Baghbadrani, and Aslani (2014), spalling was witnessed for specimens subjected to temperatures more than 300 °C. The spalling varied from slight aggregate spalling (characterized by surface pitting) to significant apportions of specimens being blustered off with explosive force.
- iv. The compressive strength of specimens fell notably for both normal concrete and NSHA blended concrete samples when exposed to the temperature exceeding 400 °C. The drop in compressive strength of about 60% and 69% was observed at 800 °C for the 7 and 28 days cured specimens respectively.



- v. Grounded in the investigated strength and physical properties of NSHA concrete, it is evident that 5% NSHA concrete performed better than control concrete for all mixtures for temperatures up to 400 °C. This implies that the reaction of pozzolans with portlandite is favored between 100 °C and 400 °C causing a considerable reduction of  $\text{Ca(OH)}_2$  content. Therefore, NSHA is worth recommended as a pozzolanic material for structural applications in concrete structures of which they will still perform at high temperatures up to 400 °C.

## 5.2 Recommendations

The physical and mechanical properties of neem seed husk ash concrete after exposure to elevated temperatures were investigated. Employing NSHA in concrete was observed to result in improved fire resistance. The mineralogical composition of the processed pozzolanic material was observed to vary with increasing the calcination temperature. However, it is believed that the behavior of concrete varies with the properties of ingredients used, curing conditions, heating rates, and cooling methods. Therefore, to have clear information about the new material (NSHA) as a concrete ingredient, the current study recommends the following;

- i. The influence of heating rate in calcining the neem seed husks needs to be investigated in relation to phase transformation of the NSHA produced.
- ii. The properties of NSHA concrete were investigated for a fixed heating rate; further studies could be done to investigate the same properties at different heating rates.
- iii. The real fire accidents are usually extinguished by spraying water to the burning structures, this study suggests an extended assessment of properties of NSHA concrete employing a rapid cooling technique.
- iv. The microstructural properties of NSHA concrete need to be done to properly describe transformations in micro-scale which result in altered macro properties of fired concrete.
- v. Durability studies of the blended concrete subjected to elevated temperatures may be considered for future works.

- vi. An opportunity cost study on competing uses of neem seed husks needs to be done and suggest suitable ways of ensuring their availability.

## REFERENCES

- Abid, M., Hou, X., Zheng, W., & Hussain, R. R. (2017). High temperature and residual properties of reactive powder concrete – A review. *Construction and Building Materials*, 147, 339-351. doi: 10.1016/j.conbuildmat.2017.04.083.
- Adebisi, J. A., Agunsoye, J. O., Bello, S. A., Kolawole, F. O., Ramakokovhu, M. M., Daramola, M. O., & Hassan, S. B. (2019). Extraction of silica from sugarcane bagasse, cassava periderm and maize stalk: Proximate analysis and physico-chemical properties of wastes. *Waste and Biomass Valorization*, 10(3), 617-629. doi: 10.1007/s12649-017-0089-5.
- Adesanya, D. A., & Raheem, A. A. (2009). Development of corn cob ash blended cement. *Construction and Building Materials*, 23(1), 347-352. doi: 10.1016/j.conbuildmat.2007.11.013.
- Ali, M. H., Mashud, M., Rubel, M. R., & Ahmad, R. H. (2013). Biodiesel from Neem oil as an alternative fuel for Diesel engines. *Procedia Engineering*, 56, 625-630. doi: 10.1016/j.proeng.2013.03.169.
- Altwait, N., Johari, M. A. M., & Hashim, S. F. S. (2011). Influence of calcination temperature on characteristics and pozzolanic activity of palm oil waste ash. *Australian Journal of Basic and Applied Sciences*, 5(11), 1010-1018. Retrieved from <http://www.ajbasweb.com/old/ajbas/2011/November-2011/1010-1018.pdf>.
- Aprianti, E., Shafigh, P., Bahri, S., & Farahani, J. N. (2015). Supplementary cementitious materials origin from agricultural wastes—A review. *Construction and Building Materials*, 74, 176-187. doi: 10.1016/j.conbuildmat.2014.10.010.
- Arioz, O. (2007). Effects of elevated temperatures on properties of concrete. *Fire Safety Journal*, 42(8), 516-522. doi: 10.1016/j.firesaf.2007.01.003.
- Aslani, F., & Bastami, M. (2011). Constitutive relationships for normal-and high-strength concrete at elevated temperatures. *American Concrete Institute Materials Journal*, 108(4), 355-364. Retrieved from [Retrieved from: //www.researchgate.net/publication/26](http://www.researchgate.net/publication/26).

- Awal, A. A., & Shehu, I. A. (2015). Performance evaluation of concrete containing high volume palm oil fuel ash exposed to elevated temperature. *Construction and Building Materials*, 76, 214-220. doi: 10.1016/j.conbuildmat.2014.12.001.
- Bahurudeen, A., Kanraj, D., Dev, V. G., & Santhanam, M. (2015). Performance evaluation of sugarcane bagasse ash blended cement in concrete. *Cement and Concrete Composites*, 59, 77-88. doi: 10.1016/j.cemconcomp.2015.03.004.
- Bastami, M., Baghbadrani, M., & Aslani, F. (2014). Performance of nano-Silica modified high strength concrete at elevated temperatures. *Construction and Building Materials*, 68, 402-408. doi: 10.1016/j.conbuildmat.2014.06.026.
- BSI. (1986). BS 1881:Part 125: Methods for mixing and sampling fresh concrete in the laboratory. London: British Standards Institution.
- BSI. (2009). BS EN 12390-3: 2009: Testing hardened concrete. Compressive strength of test specimens. UK: BSI London.
- Butler, W. B., & Kanare, H. M. (1988). Testing Fly Ash for Fineness to ASTM C 430: Sieve Calibration. *MRS Online Proceedings Library Archive*, 136, 107. doi: 10.1557/PROC-136-107.
- Chen, B., Li, C., & Chen, L. (2009). Experimental study of mechanical properties of normal-strength concrete exposed to high temperatures at an early age. *Fire Safety Journal*, 44(7), 997-1002. doi: 10.1016/j.firesaf.2009.06.007.
- Daniel, K., & Sanjayan, J. G. (2010). Effect of elevated temperatures on geopolymer paste, mortar, and concrete. *Cement and Concrete Research*, 40(2), 334-339. doi: 10.1016/j.cemconres.2009.10.017.
- Duggal, S. K. (2008). *Building Materials* (3<sup>rd</sup> ed.). New Delhi: New Age International (P) Ltd.
- Ejeh, S., Abubakar, I., Ocholi, A., & Nurudeen, M. (2014). Effect of Neem Seed Husk Ash on Concrete Strength Properties. *Nigerian Journal of Technology*, 33(2), 163-169. doi: 10.4314/njt.v33i2.4.

- EN. (2002). 1991-1-2: Eurocode 1, Part 1-2: Actions on structures: general actions—actions on the structures exposed to fire. CEN, Bruxelles, Belgique.
- EN, B. (1992). BS 882:1992: Specification for aggregates from natural sources for concrete. London: British Standards Institution.
- Fang, G., Ho, W. K., Tu, W., & Zhang, M. (2018). Workability and mechanical properties of alkali-activated fly ash-slag concrete cured at ambient temperature. *Construction and Building Materials*, 172, 476-487. doi: 10.1016/j.conbuildmat.2018.04.008.
- Fares, H., Noumowe, A., & Remond, S. (2009). Self-consolidating concrete subjected to high temperature: mechanical and physicochemical properties. *Cement and Concrete Research*, 39(12), 1230-1238. doi: 10.1016/j.cemconres.2009.08.001.
- Gambhir, M. L. (2013). *Concrete Technology: Theory and Practice* (5<sup>th</sup> ed.). New Delhi: Tata McGraw-Hill Education.
- Gar, P. S., Suresh, N., & Bindiganavile, V. (2017). Sugar cane bagasse ash as a pozzolanic admixture in concrete for resistance to sustained elevated temperatures. *Construction and Building Materials*, 153, 929-936. doi: 10.1016/j.conbuildmat.2017.07.107.
- Gartner, E. M., Young, J. F., Damidot, D. A., & Jawed, I. (2002). Hydration of Portland cement: *Structure and Performance of Cement*, 2, 57-113.
- Gursel, A. P., Maryman, H., & Ostertag, C. (2016). A life-cycle approach to environmental, mechanical, and durability properties of “green” concrete mixes with rice husk ash. *Journal of Cleaner Production*, 112, 823-836. doi: 10.1016/j.jclepro.2015.06.029.
- Hager, I. (2013). Behaviour of cement concrete at high temperature. *Bulletin of the Polish Academy of Sciences: Technical Sciences*, 61(1), 145-154. doi: 10.2478/bpasts-2013-0013.
- Haloob, M. K. (2011). Effects of Exposure to Elevated Temperatures on Properties of Concrete Containing Rice Husk Ash (Masters thesis, Universiti Sains Malaysia, Malaysia). Retrieved from <https://www.researchgate.net/publication/296706983>.

- Horszczaruk, E., Sikora, P., Cendrowski, K., & Mijowska, E. (2017). The effect of elevated temperature on the properties of cement mortars containing nano-silica and heavyweight aggregates. *Construction and Building Materials*, 137, 420-431. doi: 10.1016/j.conbuildmat.2017.02.003.
- Ibiwoye, E., & Naalla, A. (2017). Effect of Neem Seed Husk Ash on the Workability of Concrete. *TETFUND Sponsored Kwara state Polytechnic Journal of Research and Development Studies*, 11(1), 1-11. Retrieved from <https://kwarastatepolytechnic.edu.ng>.
- Ishak, S., Lee, H. S., Singh, J. K., Ariffin, M. A. M., Lim, N. H. A. S., & Yang, H. M. (2019). Performance of Fly Ash Geopolymer Concrete Incorporating Bamboo Ash at Elevated Temperature. *Materials*, 12(20), 3404. doi: 10.3390/ma12203404.
- Ismail, M., Ismail, M. E., & Muhammad, B. (2011). Influence of elevated temperatures on physical and compressive strength properties of concrete containing palm oil fuel ash. *Construction and Building Materials*, 25(5), 2358-2364. doi: 10.1016/j.conbuildmat.2010.11.034.
- Janotka, I., & Nürnbergerová, T. (2005). Effect of temperature on the structural quality of the cement paste and high-strength concrete with silica fume. *Nuclear Engineering and design*, 235(17-19), 2019-2032. doi: 10.1016/j.nucengdes.2005.05.011.
- Khaliq, W., & Mujeeb, A. (2019). Effect of processed pozzolans on residual mechanical properties and macrostructure of high-strength concrete at elevated temperatures. *Structural Concrete*, 20(1), 307-317. doi: 10.1002/suco.201800074.
- Khoury, G. (1992). Compressive strength of concrete at high temperatures: a reassessment. *Magazine of Concrete Research*, 44(161), 291-309. doi: 10.1680/mac.1992.44.161.291.
- Khoury, G. A. (2000). Effect of fire on concrete and concrete structures. *Progress in Structural Engineering and Materials*, 2(4), 429-447. doi: 10.1002/pse.51.
- Kodur, V. (2014). Properties of concrete at elevated temperatures. *International Scholarly Research Network Civil Engineering*, 2014, 1-15. doi: 10.1155/2014/468510.

- Kong, Huang, S., Corr, D., Yang, Y., & Shah, S. P. (2018). Whether do nano-particles act as nucleation sites for CSH gel growth during cement hydration? *Cement and Concrete Composites*, 87, 98-109. doi: 10.1016/j.cemconcomp.2017.12.007.
- Kurdowski, W. (2014). *Cement and Concrete Chemistry*. New York, London: Springer Dordrecht Heidelberg.
- Li, Z. (2011). *Advanced Concrete Technology*. New Jersey: John Wiley & Sons, Inc.
- Ma, Q., Guo, R., Zhao, Z., Lin, Z., & He, K. (2015). Mechanical properties of concrete at high temperature review. *Construction and Building Materials*, 93, 371-383. doi: 10.1016/j.conbuildmat.2015.05.131.
- Mboya, H. A., King'onde, C. K., Njau, K. N., & Mrema, A. L. (2017). Measurement of pozzolanic activity index of scoria, pumice, and rice husk ash as potential supplementary cementitious materials for Portland cement. *Advances in Civil Engineering*, 2017, 13. doi: 10.1155/2017/6952645.
- Mehta, P. K., & Monteiro, P. J. (2017). *Concrete Microstructure, Properties, and Materials* (2<sup>nd</sup> ed.). Berkeley: University of California.
- Morsy, M. S., Alsayed, S. H., & Aqel, M. (2010). Effect of elevated temperature on mechanical properties and microstructure of silica flour concrete. *International Journal of Civil & Environmental Engineering*, 10(1), 1-6. doi: 10.8e60/c25081c.
- Musa, N. M. (2013). Influence of neem seed husk ash on the tensile strength of concrete. *American Journal of Engineering Research*, 12, 171-174. Retrieved from [http://www.ajer.org/papers/v2\(12\)/T0212171174.pdf](http://www.ajer.org/papers/v2(12)/T0212171174.pdf).
- Musa, N. M. (2014). Thermal analysis of cement, partially replaced with Neem Seed Husk Ash. *International Journal of Scientific and Engineering Research*, 5(1), 1101-1105. Retrieved from <http://citeseerx.ist.psu.edu/viewdoc/download?doi=10.1.1.429.3080&rep>.

- Musa, N. M., & Ejeh, S. P. (2012). Synergic effect of neem seed husk ash on strength properties of cement-sand mortar. *International Journal of Engineering Research and Applications*, 2(5), 27-30. Retrieved from <https://www.ijera.com/papers/Vol2 issue5 /G2>.
- Naqi, A., & Jang, J. G. (2019). Recent progress in green cement technology utilizing low-carbon emission fuels and raw materials: A review. *Sustainability*, 11(2), 537. doi: 10.3390/su11020537.
- Neville, A. M., & Brooks, J. J. (2010). *Concrete Technology* (2<sup>nd</sup> ed.). Harlow, England: Pearson Education Limited.
- Noumowe, A. (2005). Mechanical properties and microstructure of high strength concrete containing polypropylene fibres exposed to temperatures up to 200 °C. *Cement and Concrete Research*, 35(11), 2192-2198. doi: 10.1016/j.cemconres.2005.03.007.
- Owaid, H. M., Hamid, R., & Taha, M. R. (2016). Elevated Temperature Performance of Multiple-Blended Binder Concretes. In S. Yilmaz & H. B. Ozmen (Eds.), *High Performance Concrete Technology and Applications* (pp. 87-112): IntechOpen.
- Parthasarathi, N., Saraf, D. S., Prakash, M., & Satyanarayanan, K. (2019). Analytical and experimental study of the reinforced concrete specimen under elevated temperature. *Materials Today: Proceedings*, 14, 195-201. doi: 10.1016/j.matpr.2019.04.138.
- Potha Raju, M., Shobha, M., & Rambabu, K. (2004). Flexural strength of fly ash concrete under elevated temperatures. *Magazine of Concrete Research*, 56(2), 83-88. doi: 10.1680/mac.2004.56.2.83.
- Raheem, A. A., & Ibiwoye, E. O. (2018). A Study of Neem Seed Husk Ash as Partial Replacement for Cement in Concrete. *International Journal of Sustainable Construction Engineering and Technology*, 9(2), 55-65. Retrieved from <https://publisher.uthm.edu.my/ojs/index.php/IJSCET/article/view/1534>.
- Ramesh, K. V., Raju, M. D., & Rekha, K. (2016). A Study on High Volume Fly Ash Concrete Exposed To Elevated Temperatures. *American Journal of Engineering Research*, 5(11), 227-238. Retrieved from <https://www.academia.edu/30011069/>.



- Rashad, A. M. (2015). An investigation of high-volume fly ash concrete blended with slag subjected to elevated temperatures. *Journal of Cleaner Production*, 93, 47-55. doi: 10.1016/j.jclepro.2015.01.031.
- Savva, A., Manita, P., & Sideris, K. (2005). Influence of elevated temperatures on the mechanical properties of blended cement concretes prepared with limestone and siliceous aggregates. *Cement and Concrete Composites*, 27(2), 239-248. doi: 10.1016/j.cemconcomp.2004.02.013.
- Scrivener, K. L., Juilland, P., & Monteiro, P. J. (2015). Advances in understanding the hydration of Portland cement. *Cement and Concrete Research*, 78, 38-56. doi: 10.1016/j.cemconres.2015.05.025.
- Shetty, M. S. (2000). *Concrete Technology: Theory and Practice*. New Delhi: S. Chandi & Company LTD.
- Soares, M. M. N., Poggiali, F. S., Bezerra, A. C. S., Figueiredo, R. B., Aguilar, M. T. P., & Cetlin, P. R. (2014). The effect of calcination conditions on the physical and chemical characteristics of sugar cane bagasse ash. *Rem: Revista Escola de Minas*, 67(1), 33-39. doi: 10.1590/S0370-44672014000100005.
- Tangchirapat, W., Saeting, T., Jaturapitakkul, C., Kiattikomol, K., & Siripanichgorn, A. (2007). Use of waste ash from palm oil industry in concrete. *Waste Management*, 27(1), 81-88. doi: 10.1016/j.wasman.2005.12.014.
- Turner, L. K., & Collins, F. G. (2013). Carbon dioxide equivalent (CO<sub>2</sub>-e) emissions: A comparison between geopolymer and OPC cement concrete. *Construction and Building Materials*, 43, 125-130. doi: 10.1016/j.conbuildmat.2013.01.023.
- Umasabor, R., & Okovido, J. (2018). Fire resistance evaluation of rice husk ash concrete. *Heliyon*, 4(12), e01035. doi: 10.1016/j.heliyon.2018.e01035.
- Wang, W., Meng, Y., & Wang, D. (2017). Effect of Rice Husk Ash on High-Temperature Mechanical Properties and Microstructure of Concrete. *Kemija u Industriji*, 66(3-4), 157-164. doi: 10.15255/KUI.2016.054.

Xu, Y., Wong, Y., Poon, C., & Anson, M. (2001). Impact of high temperature on PFA concrete. *Cement and Concrete Research*, 31(7), 1065-1073. doi: 10.1016/S0008-8846(01)00513-0.

## APPENDICES

### Appendix 1: Preparation of NSHA



Appendix 2: Moisture content and bulk density of aggregates

MOISTURE CONTENT

Specimen reference		Coarse Aggregates	Fine Aggregates
Container no.	unit	A1	A2
Mass of wet sample + container	g	212.90	220.90
Mass of dry sample + container	g	208.11	213.75
Mass of container	g	70.33	70.50
Mass of moisture	g	4.79	7.15
Mass of dry sample	g	137.78	143.25
<b>MOISTURE CONTENT</b>	<b>%</b>	<b>3.48</b>	<b>4.99</b>

BULK DENSITY

Length of cylinder	$l_1$	cm	12.70	12.70
Sample to edge	$l_2$	cm	0.00	0.00
Sample to edge	$l_3$	cm	0.00	0.00
Length of sample	$L=l_1-l_2-l_3$	cm	12.70	12.70
Internal diameter	D	cm	10	10
Area of sample	$A=\frac{\pi}{4} \times D^2$	cm <sup>2</sup>	78.57	78.57
Volume of sample	$V=L \times A$	cm <sup>3</sup>	997.86	997.86
Mass of cylinder + sample	$m_T$	g	2388.65	2513.5
Mass of cylinder	$m_c$	g	926.8	926.8
Mass of sample	$M=m_T-m_c$	g	1461.87	1586.72
<b>BULK DENSITY</b>	$\rho=\frac{M}{V} \times 1000$	<b>kg/m<sup>3</sup></b>	<b>1465.01</b>	<b>1590.13</b>

Appendix 3: Water absorption and the specific gravity of aggregates

WATER ABSORPTION			
<b>Specimen reference</b>	<b>Unit</b>	<b>Coarse Aggregates</b>	<b>Fine Aggregates</b>
Mass of saturated surface dry aggregate in air	g	515.59	520.10
Mass of oven-dry aggregate in air	g	507.20	510.45
Water Absorption	%	<b>1.65</b>	<b>1.89</b>

SPECIFIC GRAVITY			
Weight of empty pycnometer, $W1$	g	667.50	667.50
Weight of pycnometer half filled with sand, $W2$	g	1352.5	1347.4
Weight of pycnometer filled with half sand and half water, $W3$	g	1988.6	1957.6
Weight of pycnometer filled with water, $W4$	g	1523.1	1523.1
SPECIF GRAVITY, $G_s$		<b>3.12</b>	<b>2.77</b>

#### Appendix 4: Particle size distribution of aggregates

Sieve size (mm)	Coarse aggregates		Fine aggregates	
	Cumulative mass retained (g)	% Passing	Cumulative mass retained (g)	% Passing
37.5	0	100	0	100
19	58.1	99.8	3035.6	99.5
9.5	105.1	99.6	11494.3	99.2
4.75	224.9	99.1	12517.3	98.2
2.36	425.2	98.2	12564.8	96.6
1.18	871.2	96.3	12591.8	93.1
0.6	2143.5	91.0	12616.9	83.1
0.3	5381.4	77.4	12661.3	57.6
0.15	7118.8	70.1	12702.3	44.0
0.075	7483.6	68.6	12712.4	41.2

## Appendix 5: Detailed concrete mix design calculations

### Stage 1: Selection of targeted ratio of water to cement

From Table 9, the compressive strength for the mix made of OPC (type II) and water to cement ratio of 0.50 is 49 MPa. It follows that, from Fig. 22, the free water to cement ratio for the required mean compressive strength of 49 MPa is 0.58. Therefore, the lower water to cement ratio will be used.

Table 9: Approximate compressive strengths (N/mm<sup>2</sup>) of concrete mixes made with a free water/cement ratio of 0.5

Cement strength class	Type of coarse aggregate	Compressive strengths (N/mm <sup>2</sup> )			
		Age (days)			
		3	7	28	91
42.5	Uncrushed	22	30	42	49
	Crushed	27	36	49	56
52.5	Uncrushed	29	37	48	54
	Crushed	34	43	55	61

Throughout this publication concrete strength is expressed in the units N/mm<sup>2</sup>.  
 1 N/mm<sup>2</sup> = 1 MN/m<sup>2</sup> = 1 MPa. (N = newton; Pa = pascal.)

BSI (1986) – Table 2.

Considering 5% defectiveness and for less than 20 samples per batch, the margin strength can be calculated as follows;

Margin strength = standard deviation (from Fig. 21) × appropriate defectiveness value

$$= 8 \times 1.64$$

$$= 13.12$$

The target mean strength = specified mean strength + the margin

$$= 25 + 13.12 = 38.12 \text{ MPa}$$

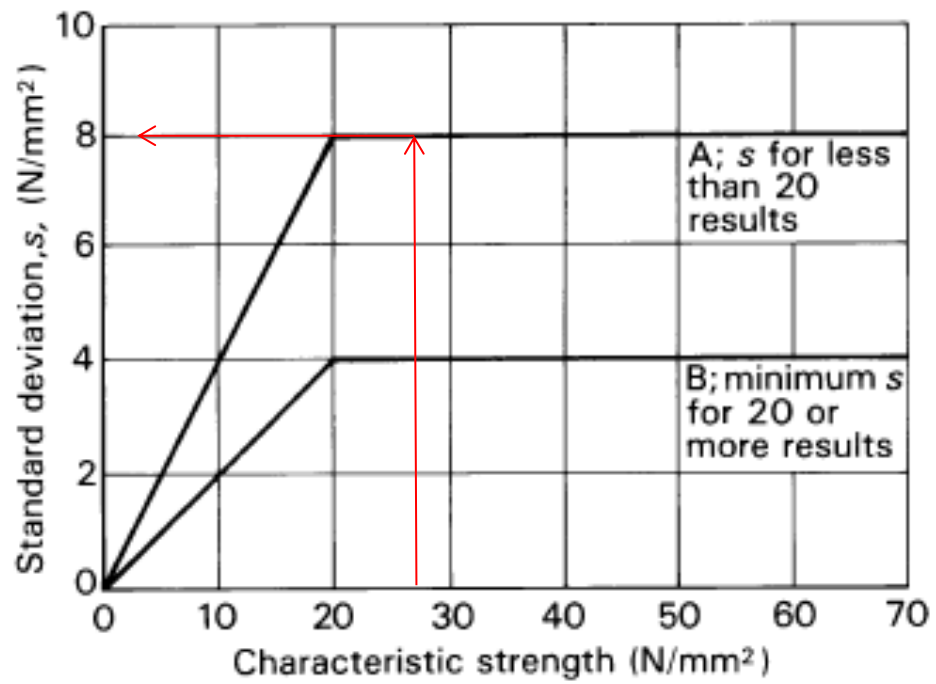


Figure 21: Relationship between standard deviation and characteristic strength; BSI (1986) – Fig. 3



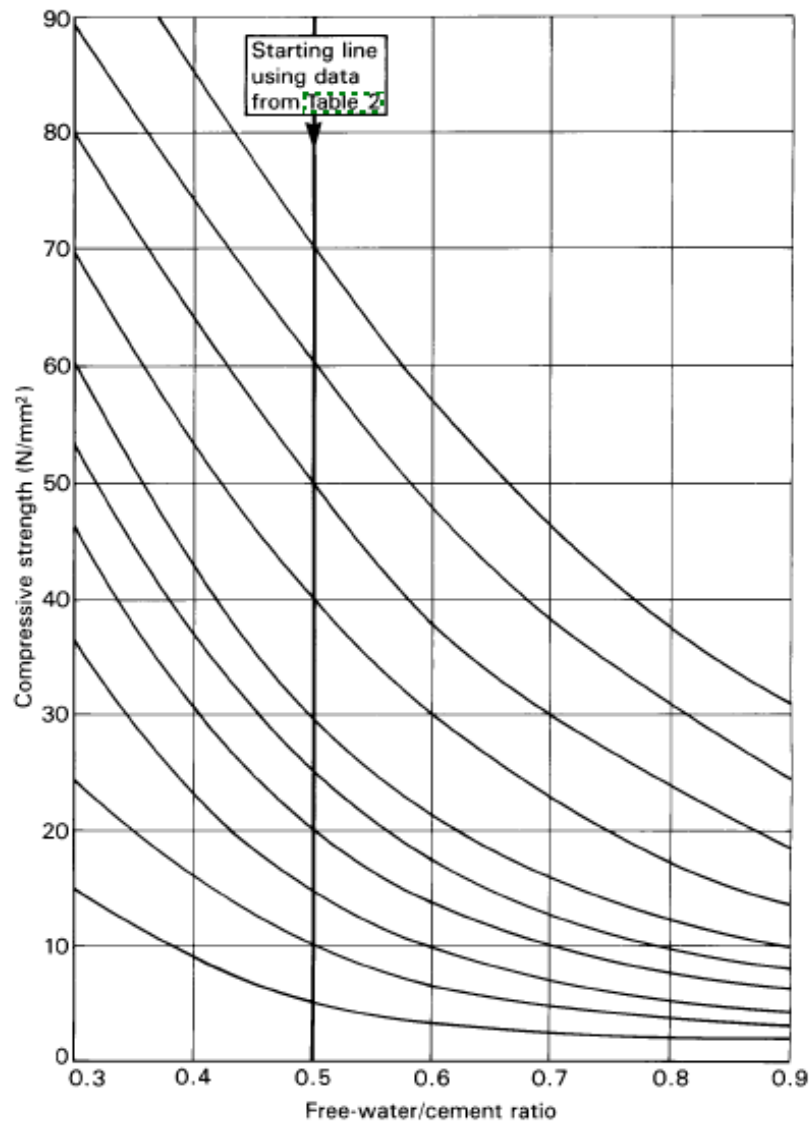


Figure 22: Relationship between compressive strength and free-water/cement ratio; BSI (1986) – Fig. 4

## Stage 2: Selection of free water content

From Table 10, the approximate workability requires a slump in a range of 60 - 180 mm so that the amount of free water required for crushed coarse aggregate with 20 mm maximum size of and the uncrushed fine aggregates is  $\frac{2}{3}(195) + \frac{1}{3}(225) = 205 \text{ kg/m}^3$  of concrete.

Table 10: Approximate free-water contents (kg/m<sup>3</sup>) for various levels of workability

Slump (mm)		0-10	10-30	30-60	60-180
Vebe time (s)		>12	6-12	3-6	0-3
Maximum size of aggregate (mm)					
Type of aggregate					
10	Uncrushed	150	180	205	225
	Crushed	180	205	230	250
20	Uncrushed	135	160	180	195
	Crushed	170	190	210	225
40	Uncrushed	115	140	160	175
	Crushed	155	175	190	205

Note: When coarse and fine aggregates of different types are used, the free-water content is estimated by the expression:

$$^{2/3} W_f + ^{1/3} W_c$$

where  $W_f$  = free-water content appropriate to type of fine aggregate

and  $W_c$  = free-water content appropriate to type of coarse aggregate.

BSI (1986) – Table 3.

### Stage 3: Determination of cement content

The amount of cement is therefore  $\frac{205}{0.50} = 410$  kg/m<sup>3</sup> of concrete. According to Table 11, the minimum required cement content for moderate exposure conditions is 240 kg/m<sup>3</sup> of concrete. Thus, our estimated cement content is satisfactory.

Table 11: Minimum cement content requirement

Minimum Cement Content, Maximum Water-Cement Ratio and Minimum Grade of Concrete for Different Exposures with Normal Weight Aggregates of 20 mm Nominal Maximum Size

Exposure	Plain concrete			Reinforced concrete		
	Minimum cement content (kg/m <sup>3</sup> )	Maximum free water-cement ratio	Minimum grade of concrete	Minimum cement content (kg/m <sup>3</sup> )	Maximum free water-cement ratio	Minimum grade of concrete
Mild	220	0.60	-	300	0.55	M20
Moderate	240	0.60	M15	300	0.50	M25
Severe	250	0.50	M20	320	0.45	M30
Very severe	260	0.45	M20	340	0.45	M35
Extreme	280	0.40	M25	360	0.40	M40

BSI (1986).

#### Stage 4: Determination of total aggregate content

From Fig. 23, for aggregates with a bulk specific gravity of 2.7, and free water content of 205 kg/m<sup>3</sup>, the wet density of concrete is 2400 kg/m<sup>3</sup>. It follows that, the total aggregate content is  $2400 - (205 + 410) = 1785$  kg/m<sup>3</sup> of concrete

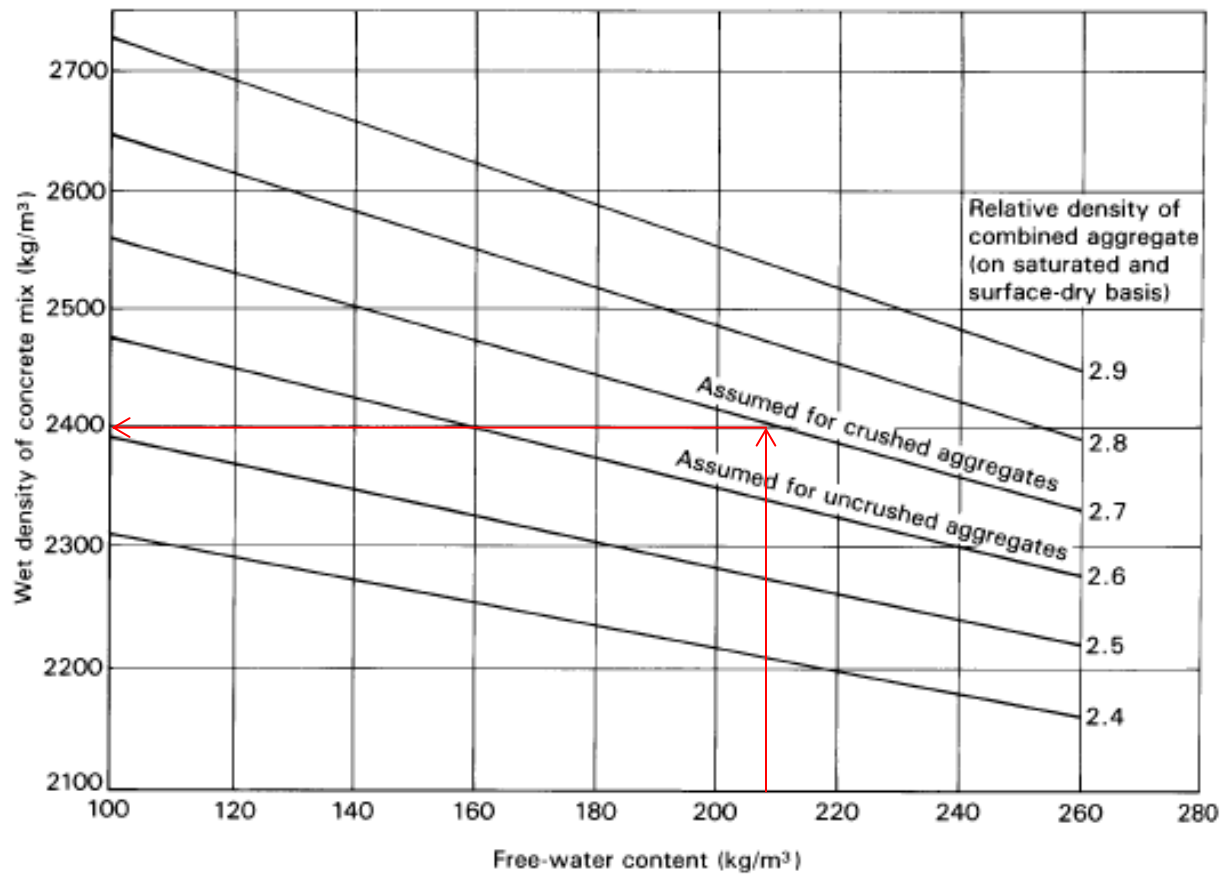


Figure 23: Estimated wet density of fully compacted concrete; BSI (1986) – Fig. 5

#### Stage 5: Selection of fine and coarse aggregate contents

For the free water to cement ratio of 0.50, a slump of 60 - 180 mm, and a maximum size of aggregate of 20 mm and the specified fineness, the fine aggregate content obtained from Fig. 24 is 30% of the total aggregate content. Hence, the fine aggregate content is  $0.3 \times 1785 = 526.58 \text{ kg/m}^3$  of concrete. The coarse aggregate content is  $1785 - 526.58 = 1258.43 \text{ kg/m}^3$  of concrete.

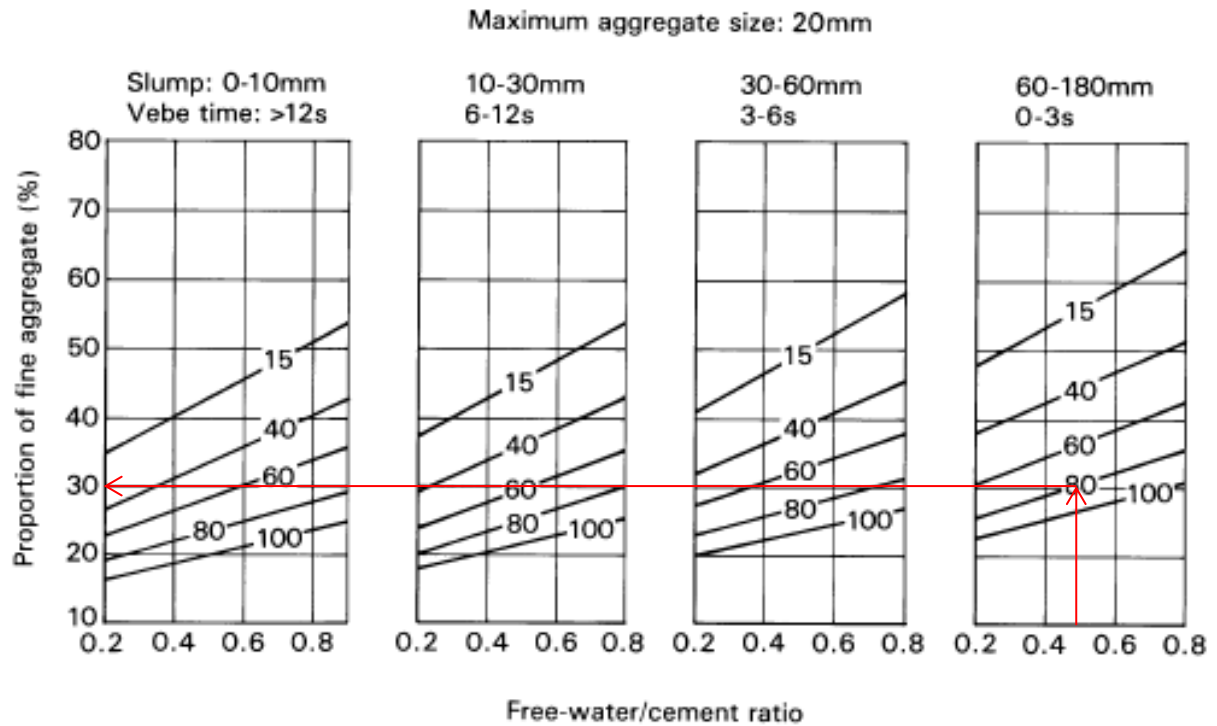


Figure 24: Recommended proportions of fine aggregate according to percentage passing a 600  $\mu\text{m}$  sieve; (BSI (1986)) – Fig.6

The estimated quantities in  $\text{kg/m}^3$  are summarized as follows;

Cement:	410
Fine aggregate:	527
Coarse aggregate:	1258
Water:	205
Total:	2400